Statistical inference in circular structural model and fitting circles to noisy data *

A. Donner† A. Goldenshluger ‡

Abstract

It is well known that commonly used algorithms for circle fitting perform poorly when sampling distribution of the points is not symmetric with respect to the circle center, e.g., when the points are sampled from a circle arc. To overcome this difficulty we introduce and study a parametric circular structural model. In this model the points are assumed to be sampled according to the von Mises distribution with unknown concentration and mean direction parameters. Under these circumstances we develop maximum likelihood and method of moments estimators of the circle center and radius, and study their statistical properties. In particular, we show that the proposed maximum likelihood estimator is asymptotically normal and efficient. We also develop a test of uniformity for the sampling distribution along the circle. Based on the derived theoretical results we propose a numerically stable circle fitting algorithm and investigate its accuracy by simulation.

Keywords: circular structural model, circle fitting, latent variables, maximum likelihood estimators, test of uniformity, von Mises distribution.

2000 AMS Subject Classification: 62F20, 65D10.

1 Introduction

The problem of circle fitting to noisy data scattered on the plane arises in such diverse areas as archaeology (Thom 1955), (Freeman 1977), microwave engineering (Delogne 1972), GPS localization (Beck & Pan 2012), robotics (Núñes et al. 2008), computer vision (Kanatani et al. 2016), to name but a few. In this problem we are given data points $\mathcal{S}_n = \{(X_i, Y_i),\ i = 1, \dots, n\}$ on the plane which are thought to be noisy versions of points on a circle, and the goal is to find the "best" circular fit to $\mathcal{S}_n$.

A natural and straightforward idea is to define an estimator $\hat{\theta} = (\hat{a}, \hat{b}, \hat{\rho})$ of the circle parameters $\theta = (a, b, \rho)$ as solution to the optimization problem

$$\hat{\theta} = \arg\min_{a,b,\rho} \sum_{i=1}^{n} \left[(X_i - a)^2 + (Y_i - b)^2 - \rho^2\right]^2, \tag{1.1}$$

where (a, b) is the circle center and ρ is its radius. This method is called the *algebraic fit*, and it is routinely used in practice. The optimization problem in (1.1) is reduced to the standard linear least squares problem and solved efficiently. Another popular circle fitting algorithm is the *geometric fit* which is defined as solution to the following optimization problem:

$$\tilde{\theta} = \arg\min_{a,b,\rho} \sum_{i=1}^{n} \left[\sqrt{(X_i - a)^2 + (Y_i - b)^2} - \rho\right]^2. \tag{1.2}$$

The optimization problem in (1.2) is a non–linear least squares problem; it is non–convex, and it is typically solved using the Gauss–Newton, Levenberg–Marquardt or specially developed algorithms [see, e.g., Beck & Pan (2012)]. Both *algebraic* and *geometric* fits work well in practice when the distribution

*The research is supported by the ISF grant 220/21

†Department of Statistics, University of Haifa, Haifa 31905, Israel. e-mail: *adonner@campus.haifa.ac.il.*

‡Department of Statistics, University of Haifa, Haifa 31905, Israel. e-mail: *goldensh@stat.haifa.ac.il.*

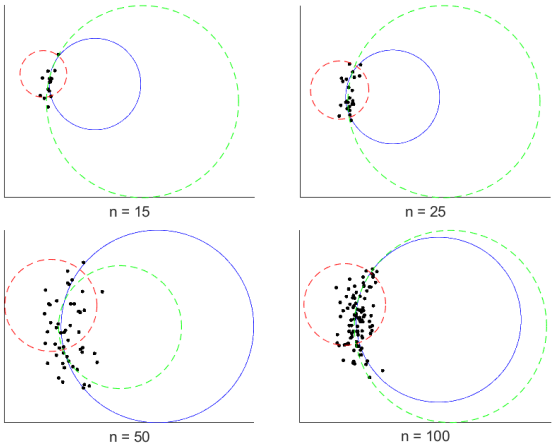

Figure 1: *The algebraic (red dashed line) and geometric (green dashed line) fits fail to estimate the true circle (blue line) when noisy observations (black dots) are sampled from a circular arc*

of the noisy data points along the circle is close to uniform, or if it is symmetric with respect to the circle center. However, in many practical situations, e.g., in computer vision applications, it is required to fit a circle to the data points which are sampled from an arc of the circle [see, e.g., Pratt (1987) and Landau (1987)]. Under these circumstances, performance of the *algebraic* and *geometric* fits is poor, and their accuracy does not improve as sample size n increases. A typical situation is displayed in Figure 1.

The main difficulty in the circle fitting problem is the presence of latent variables that determine sampling design along the circumference; the number of these variables grows with sample size. In mathematical terms the problem of circle fitting can be formulated as follows. We are given observations $\mathcal{S}_n = \{(X_i, Y_i),\ i = 1, \dots, n\}$ generated by the equations

$$\begin{aligned} X_i &= a + \rho \cos \varphi_i + \xi_i \\ Y_i &= b + \rho \sin \varphi_i + \eta_i, \end{aligned} \tag{1.3}$$

where $\varphi_i \in [0, 2\pi)$, $i = 1, \dots, n$ are unobservable angles, and (ξ_i, η_i), $i = 1, \dots, n$ are independent bivariate normal random variables with zero mean and covariance matrix $\sigma^2 I$ which represent measurement errors. The problem is to estimate the circle center (a, b) and radius ρ from observations $\mathcal{S}_n$.

There are two common approaches for modeling latent variables $\{\varphi_i, i = 1, \dots, n\}$. First, one can regard $\{\varphi_i\}$ as unknown deterministic nuisance parameters; this assumption leads to the *circular functional model*. In this model the number of nuisance parameters grows with sample size, and the classical work of Neyman & Scott (1948) shows that the maximum likelihood estimators can fail to be consistent under these circumstances [see also Kiefer & Wofowitz (1956)]. Second, $\{\varphi_i\}$ can be assumed to be independent identically distributed random variables with some distribution G on $[0, 2\pi)$. The latter assumption leads to the *circular structural model* which is a mixture model with mixing nuisance distribution G [see, e.g., Lindsay (1980)]. In this paper we focus on statistical inference in the circular structural model when nuisance distribution G belongs to the parametric family of von Mises distributions with unknown concentration and mean direction parameters.

Related literature. The problem of circle fitting is a subject of considerable literature; for a book–length survey of the area we refer to Chernov (2010). Below we provide a brief review of existing results that are most relevant to our work.

Majority of existing literature deals with numerical aspects of circle fitting and associated optimization problems. The most common approach for solving the geometric fit optimization problem (1.2) is the Levenberg-Marquardt algorithm. In addition, some special methods for solution of (1.2) have been developed. In particular, Landau (1987) suggested an iterative two step minimization algorithm, where the objective function is first minimized with respect to ρ for fixed a, b, and then with respect to a and b with the plugged–in current value of ρ. Similar approach was suggested by Späth (1996), but with

a different parameterization. Kåsa (2011) suggested a simplistic approach for solving the algebraic fit problem (1.1) by reducing it to a standard linear least squares problem. These methods perform well when the data are almost noise–free, i.e., noise variance σ^2 is close to zero. However, for larger values of σ^2 these methods perform poorly when the observations are spread across less than half a circle. Motivated by this difficulty, Chernov & Ososkov (1984) suggested an approximation to the objective function of the geometric fit optimization problem. Specifically, the approximation is given by

$$\sum_{i=1}^{n} \left(\sqrt{(X_i - a)^2 + (Y_i - b)^2} - \rho \right)^2 \approx \frac{1}{4\rho^2} \sum_{i=1}^{n} \left((X_i - a)^2 + (Y_i - b)^2 - \rho^2 \right)^2, \tag{1.4}$$

and it involves the objective function of the algebraic fit problem multiplied by factor $(2\rho)^{-2}$. The right hand side of (1.4) can be efficiently minimized numerically. The suggested method yields better results when the data scattered across a small circular arc. Pratt (1987) and Taubin (1991) considered the same approximation (1.4) but with the algebraic parameterization of the circle equation, $A(x^2 + y^2) + Bx + Cy + D = 0$, which, with an additional constraint, provides an one–to–one mapping to the representation with parameters a, b, ρ. Both the Pratt and Taubin fits are represented as quadratic optimization problems and solved efficiently. Hence both approaches are very common and sometimes their results serve as initial points for iterative solution of the geometric fit problem.

In contrast to numerical aspects, statistical properties of circle fitting algorithms have been studied to a much lesser extent. Chan (1965) investigated the circular functional model (1.3), where unobservable angles φ_i, $i = 1, \ldots, n$ are treated as unknown deterministic nuisance parameters. It is shown in the aforementioned paper that the maximum likelihood (ML) estimation of all parameters in this model (including nuisance parameters) leads to the geometric fit algorithm. Chan (1965) proved that necessary and sufficient conditions for consistency of the ML estimator of the circle center (a, b) are

$$\lim_{n\to\infty} \sum_{i=1}^{n} \cos\varphi_i = \lim_{n\to\infty} \sum_{i=1}^{n} \sin\varphi_i = 0. \tag{1.5}$$

The meaning of (1.5) is that unobservable angles are distributed symmetrically with respect to the circle center in asymptotics as $n \to \infty$. In what follows we refer to (1.5) as the *symmetry conditions*. Chernov (2011) showed that under the same assumptions as in Chan (1965), the ML estimators of the circle parameters have infinite expectation. Similar phenomenon holds in the functional linear regression model; see Anderson (1976). Berman & Culpin (1986) studied asymptotic bias of the algebraic fit estimators and showed that the bias converges to zero as $n \to \infty$ if and only if the symmetry conditions (1.5) hold. Kanatani & Rangarajan (2011) and Al-Sharadqah & Chernov (2009) considered both the algebraic and geometric fit estimators, and studied their mean squared errors in small noise asymptotics as $\sigma^2 \to 0$ and sample size n is fixed. Under these circumstances, both the algebraic and geometric fit estimators are consistent. Anderson (1981) introduced the circular structural model (1.3), where unobservable angles $\{\varphi_i\}$ are assumed to follow the uniform distribution on $[0, 2\pi)$. Anderson (1981) derived estimating equations for the ML estimators in the considered setting and discussed some of their properties. It is worth mentioning that in the setting of Anderson (1981) the symmetry conditions (1.5) hold (the convergence in (1.5) should be understood as convergence in probability). Therefore both algebraic and geometric fit estimators are consistent.

The above brief review of existing literature shows that very little is known about statistical properties of circle fitting algorithms in the situation when the sampling distribution of angles is non–symmetric with respect to the circle center. In this paper we propose a parametric statistical model that allows non–symmetric sampling, solve related statistical inference problems for this model, and develop a numerically stable circle fitting algorithm with provable theoretical accuracy guarantees.

The paper contributions. In this paper our goal is two–fold. First, we propose a parametric circular structural model when the unobservable angle variables $\{\varphi_i\}$ in (1.3) follow the von Mises distribution on the circle. The von Mises distribution is a unimodal distribution that is commonly used in modeling circular data [see, e.g., Mardia & Jupp (2000)]. We study asymptotic properties of the ML estimators in the proposed model and show that they are asymptotically normal and efficient. Motivated by numerical difficulties in implementation of the ML estimators, we also develop the method of moments estimators of the circle parameters and propose a test of uniformity for the sampling distribution in the circular

structural model. The test of uniformity is a part of the proposed circle fitting algorithm; it is also of independent interest. Second, based on the derived theoretical results, a stable numerical algorithm for estimating the circle parameters is developed. The circle fitting algorithm works under broad conditions; it uses the method of moments estimates as initial points, and utilizes the uniformity test for efficient solution of the ML optimization problem. We illustrate performance of the proposed algorithm using extensive simulation experiments and compare it with the existing state–of-the–art circle fitting algorithms.

Organization. The rest of the paper is structured as follows. Section 2 presents the suggested parametric model along with discussion of its identifiability. Section 3 deals with the ML estimation in the circular structural model. Section 4 contains detailed development of the method of moments estimators. In Section 5 we develop a test of uniformity for the angle distribution in the circular structural model. Finally, Section 6 presents our final circle fitting algorithm, discusses its implementation and reports on results of an extensive simulation study. Appendix A collects some known facts and results about the von Mises distribution and the modified Bessel functions of first kind. These facts are extensively used in the paper. The proofs of all results are given in Appendix B.

Notation. The following notation is used throughout the paper. The symbol $\mathbb{E}_\theta$ stands for the expectation with respect to the probability measure $\mathbb{P}_\theta$ of observations when the unknown parameter of the circular structural model is θ. The modified Bessel function of the first kind of order k is denoted $I_k(z)$, $z \in \mathbb{C}$. The ratios of the Bessel functions appear frequently in our calculations; we denote $R_k(z) := I_k(z)/I_0(z)$, $k = 0, \pm 1, \ldots$. For random variable φ having von Mises distribution with concentration $\varkappa \geq 0$ and mean direction $\mu \in [0, 2\pi)$ we write $\varphi \sim \mathrm{vM}(\mu, \varkappa)$. The density of the von Mises distribution is denoted

$$g(\varphi) = \frac{e^{\varkappa \cos(\varphi - \mu)}}{2\pi I_0(\varkappa)}, \quad \varphi \in [0, 2\pi). \tag{1.6}$$

2 Circular structural model

The suggested model we discuss in this paper is the structural version of (1.3). We assume that the available observations (X_i, Y_i), $i = 1, \ldots, n$ are generated by equations

$$X_i = a + \rho \cos \varphi_i + \xi_i \tag{2.1}$$
$$Y_i = b + \rho \sin \varphi_i + \eta_i, \tag{2.2}$$

where (a, b) and $\rho > 0$ are the circle center and radius respectively, $(\xi_i, \eta_i) \sim \mathcal{N}_2(0, \sigma^2 I)$, $i = 1, \ldots, n$ are independent bivariate normal measurement errors, and φ_i, $i = 1, \ldots, n$ are independent identically distributed random variables, $\varphi_i \sim \mathrm{vM}(\mu, \varkappa)$. We assume that $\{\varphi_i, i = 1, \ldots, n\}$ and $\{(\xi_i, \eta_i), i = 1, \ldots, n\}$ are independent.

The introduced model is parametrized by $\theta := (a, b, \rho, \sigma^2, \mu, \varkappa)$, where a, b, and ρ are the parameters of interest, while σ^2, μ and $\varkappa$ are nuisance parameters. The joint probability density $f_\theta(x, y)$ of generic observation (X, Y) is a mixture distribution

$$\begin{aligned} f_\theta(x, y) &= \frac{1}{2\pi\sigma^2} \int_0^{2\pi} \exp\Big\{ -\frac{1}{2\sigma^2}\Big[(x - a - \rho\cos\varphi)^2 + (y - b - \rho\sin\varphi)^2\Big]\Big\} g(\varphi)\mathrm{d}\varphi \\ &= \frac{1}{2\pi\sigma^2} \exp\Big\{ -\frac{1}{2\sigma^2}\Big[(x-a)^2 + (y-b)^2 + \rho^2\Big]\Big\} \frac{I_0\big(D_\theta(x,y)\big)}{I_0(\varkappa)}, \end{aligned} \tag{2.3}$$

where we have denoted

$$D_\theta(x, y) := \sqrt{A_\theta^2(x) + B_\theta^2(y)},$$
$$A_\theta(x) := \varkappa\cos\mu + \frac{\rho}{\sigma^2}(x - a), \quad B_\theta(y) := \varkappa\sin\mu + \frac{\rho}{\sigma^2}(y - b).$$

The second line in (2.3) is obtained by substitution of (1.6), and using (A.2) from Appendix A.

The corresponding parametric model is the family of distributions $\{f_\theta : \theta \in \Theta\}$, where $\theta = (a, b, \rho, \sigma^2, \mu, \varkappa)$, and the parameter set Θ is

$$\Theta := \mathbb{R} \times \mathbb{R} \times (0, \infty) \times (0, \infty) \times [0, 2\pi) \times (0, \infty). \tag{2.4}$$

We call $\{f_\theta : \theta \in \Theta\}$ *the full circular structural model*. Note that the special case $\varkappa = 0$ is not included in the parameter set Θ, even though the value $\varkappa = 0$ belongs to the parameter set of the von Mises distribution. For $\varkappa = 0$ the von Mises distribution reduces to the uniform distribution on $[0, 2\pi)$, and the mean direction parameter μ is not identified. Here for $\theta = (a, b, \rho, \sigma^2, \mu, 0)$, $f_\theta(x, y)$ does not depend on μ,

$$f_\theta(x, y) = \frac{1}{2\pi\sigma^2} \exp\left\{ -\frac{1}{2\sigma^2}\left[(x-a)^2 + (y-b)^2 + \rho^2\right]\right\} I_0\Big(\frac{\rho}{\sigma^2}\sqrt{(x-a)^2 + (y-b)^2}\Big).$$

Thus, if the value $\varkappa = 0$ is included in the parameter set Θ, the full circular structural model becomes non–identifiable. In the case $\varkappa = 0$ the model collapses to $\{f_{\theta_0} : \theta_0 \in \Theta_0\}$, where $\theta_0 := (a, b, \rho, \sigma^2)$, and the parameter set is $\Theta_0 := \mathbb{R} \times \mathbb{R} \times (0, \infty) \times (0, \infty)$. We call $\{f_{\theta_0} : \theta_0 \in \Theta_0\}$ *the reduced circular structural model*. This model was suggested and studied by Anderson (1981).

The next statement establishes identifiability of the full model.

Proposition 2.1 *The full circular structural model $\{f_\theta : \theta \in \Theta\}$ with Θ defined in (2.4) is identifiable, i.e., for any pair of parameters $\theta_1, \theta_2 \in \Theta$ such that $\theta_1 \neq \theta_2$ one has $P_{\theta_1} \neq P_{\theta_2}$, where P_θ stands for the probability measure on $(\mathbb{R}^2, \mathcal{B}(\mathbb{R}^2))$ corresponding to f_θ.*

Because $f_\theta(x, y)$ is an analytic function of (x, y) for any $\theta \in \Theta$ [see (2.3)], Proposition 2.1 implies that for all $\theta \in \Theta$ and any $\gamma > 0$ there exists constant $c_\theta(\gamma)$ such that

$$\inf_{\|\theta - \theta'\| > \gamma} \iint \left|\sqrt{f_\theta(x, y)} - \sqrt{f_{\theta'}(x, y)}\right|^2 \mathrm{d}x\mathrm{d}y \geq c_\theta(\gamma) > 0,$$

where $\|\cdot\|$ denotes the Euclidean norm. This is a standard condition used in proofs of asymptotic effiency of parametric estimators; see Ibragimov & Hasminskii (1981).

3 Maximum likelihood estimator

It follows from (2.3) that in the full circular structural model the log–likelihood function based on the sample $S_n = \{(x_i, y_i), i = 1, \ldots, n\}$ is

$$\ell_n(\theta; S_n) := \sum_{i=1}^n \ln\left[I_0\left(D_\theta(x_i, y_i)\right)\right] - \frac{1}{2\sigma^2}\sum_{i=1}^n \left[(x_i - a)^2 + (y_i - b)^2 + \rho^2\right] - n\ln\left[I_0(\varkappa)\right] - n\ln(2\pi\sigma^2),$$

while the log–likelihood function in the reduced model is

$$\ell_{0,n}(\theta; S_n) := \sum_{i=1}^n \ln\left[I_0\left(\frac{\rho}{\sigma^2}\sqrt{(x_i - a)^2 + (y_i - b)^2}\right)\right] - \frac{1}{2\sigma^2}\sum_{i=1}^n \left[(x_i - a)^2 + (y_i - b)^2 + \rho^2\right] + n\ln(2\pi\sigma^2).$$

The ML estimator of $\theta = (a, b, \rho, \sigma^2, \mu, \varkappa)$ in the full circular structural model is defined as

$$\tilde{\theta}_n := \arg\max_{\theta \in \Theta} \ell_n(\theta; S_n), \tag{3.1}$$

where Θ is given in (2.4). The ML estimator of $\theta_0 = (a, b, \rho, \sigma^2)$ in the reduced model is

$$\tilde{\theta}_{0,n} = \arg\min_{\theta \in \Theta_0} \ell_{0,n}(\theta; S_n), \tag{3.2}$$

where $\Theta_0 = \mathbb{R} \times \mathbb{R} \times (0, \infty) \times (0, \infty)$. Some properties of $\tilde{\theta}_{0,n}$ are studied in Anderson (1981).

3.1 Asymptotic normality

First we show that the full circular structural model $\{f_\theta : \theta \in \Theta\}$ defined in (2.3)–(2.4) is *regular* in the sense of the following definition; see Ibragimov & Hasminskii (1981, Chapter 1, Section 7).

Definition 3.1 *A statistical model* $\{f_\theta : \theta \in \Theta\}$ *is called* regular *if*

(i) $f_\theta(x)$ *is a continuous function on* Θ *for almost all* x*;*

(ii) *there exists finite Fisher information* $J(\theta)$ *at each point* $\theta \in \Theta$*;*

(iii) *function* $\psi_\theta(\cdot) = \nabla_\theta[f_\theta^{1/2}(\cdot)]$ *is continuous in the* $\mathbb{L}_2$*–sense, where* ∇_θ *stands for the gradient (the vector of partial first order derivatives with respect to the components of the vector* θ*).*

First, the condition (i) holds trivially for $f_\theta(x, y)$ in (2.3). Second, differentiating the log–likelihood function $\ell_1(\theta; x, y)$ based on one observation (x, y) with respect to parameters $\theta := (a, b, \rho, \sigma^2, \mu, \varkappa)$, taking into account that $I_0'(z) = I_1(z)$ [see (A.3) in Appendix A] and using notation $R_k(z) = I_k(z)/I_0(z)$ we obtain

$$\frac{\partial \ell_1(\theta; x, y)}{\partial a} = \frac{1}{\sigma^2}(x - a)\Big(1 - \frac{R_1(D_\theta)}{D_\theta}\Big) - \frac{\rho}{\sigma^2}\Big(\frac{R_1(D_\theta)}{D_\theta}\Big)\varkappa \cos\mu, \tag{3.3}$$

$$\frac{\partial \ell_1(\theta; x, y)}{\partial b} = \frac{1}{\sigma^2}(y - b)\Big(1 - \frac{R_1(D_\theta)}{D_\theta}\Big) - \frac{\rho}{\sigma^2}\Big(\frac{R_1(D_\theta)}{D_\theta}\Big)\varkappa \sin\mu, \tag{3.4}$$

$$\frac{\partial \ell_1(\theta; x, y)}{\partial \rho} = \frac{R_1(D_\theta)}{\sigma^2 D_\theta}\Big\{\frac{\rho}{\sigma^2}\big[(x - a)^2 + (y - b)^2\big] + \varkappa\big[(x - a)\cos\mu + (y - b)\sin\mu\big]\Big\} - \frac{\rho}{\sigma^2}, \tag{3.5}$$

$$\begin{aligned}\frac{\partial \ell_1(\theta; x, y)}{\partial \sigma^2} &= \frac{1}{\sigma^4}\big[(x - a)^2 + (y - b)^2\big]\Big(\frac{1}{2} - \frac{\rho^2 R_1(D_\theta)}{\sigma^2 D_\theta}\Big) \\ &\quad + \frac{\rho}{\sigma^4}\Big(\frac{1}{2} - \frac{R_1(D_\theta)}{D_\theta}\varkappa\big[(x - a)\cos\mu + (y - b)\sin\mu\big]\Big),\end{aligned} \tag{3.6}$$

$$\frac{\partial \ell_1(\theta; x, y)}{\partial \mu} = \frac{R_1(D_\theta)}{D_\theta}\frac{\varkappa\rho}{\sigma^2}\big[-(x - a)\sin\mu + (y - b)\cos\mu\big], \tag{3.7}$$

$$\frac{\partial \ell_1(\theta; x, y)}{\partial \varkappa} = -R_1(\varkappa) + \frac{R_1(D_\theta)}{D_\theta}\Big\{\varkappa^2 + \frac{\rho}{\sigma^2}\big[(x - a)\cos\mu + (y - b)\sin\mu\big]\Big\}, \tag{3.8}$$

where for brevity we write D_θ for $D_\theta(x, y)$. The Fisher information matrix is

$$J(\theta) := \mathbb{E}_\theta\Big\{\nabla_\theta\, \ell_1(\theta; X_1, Y_1)\big[\nabla_\theta\, \ell_1(\theta; X_1, Y_1)\big]^T\Big\}.$$

The finiteness of the diagonal elements of the Fisher information matrix follows from the above relationships, finiteness of all moments of (X, Y), and the fact that (Amos 1974)

$$\frac{x}{1 + \sqrt{x^2 + 1}} \le R_1(x) \le \frac{x}{\sqrt{x^2 + 4}}, \quad \forall x.$$

Therefore condition (ii) of Definition 3.1 is fulfilled. Third, function $f_\theta^{1/2}(x, y)$ is continuously differentiable with respect to $\theta \in \Theta$, so that condition (iii) also holds. Thus the model is regular in the sense of Definition 3.1.

The established regularity of the circular structural model allows us to apply powerful general theory of Ibragimov & Hasminskii (1981) for proving asymptotic optimality of ML estimators in the circular structural model. The main result of this section is given in the next statement.

Theorem 3.1 *Let* $\Theta \subset \mathbb{R}^6$ *be given in* (2.4)*, and* $J(\theta)$ *be a non–singular matrix for all* $\theta \in \Theta$*. Then for any compact set* $K \subset \Theta$ *there exists* $\epsilon > 0$ *such that with* $\mathbb{P}_\theta$*–probability one uniformly in* $\theta \in K$ *one has*

$$\sqrt{n} J(\theta)(\tilde{\theta}_n - \theta) = \frac{1}{\sqrt{n}}\sum_{j=1}^{n} \nabla_\theta\, \ell(\theta; X_i, Y_i) + O(n^{-\epsilon}), \quad n \to \infty,$$

and therefore

$$\sqrt{n}(\tilde{\theta}_n - \theta) \xrightarrow{d} \mathcal{N}(0, J^{-1}(\theta)), \quad n \to \infty.$$

Proof of Theorem 3.1 is given in Section B.2; it is based on verification of general conditions for asymptotic normality of ML estimators derived in Ibragimov & Hasminskii (1981). In fact, using results in Ibragimov & Hasminskii (1981, Section 3, Chapter III) one can prove that the family of distributions $\{f_\theta : \theta \in \Theta\}$ satisfies the LAN (local asymptotic normality) condition so that the ML estimator $\tilde{\theta}_n$ is asymptotically efficient. Our proof of Theorem 3.1 also demonstrates that the same results hold for the ML estimator in the reduced circular structural model; see (3.2). We note that although the reduced model has been studied in Anderson (1981), the cited paper does not contain results on asymptotic normality and efficiency of the associated ML estimator.

3.2 Remarks on numerical implementation

The ML estimator $\tilde{\theta}_n$ has very attractive theoretical properties. However, its numerical implementation presents several difficulties. The objective function in (3.1) is non-convex, so there are no guarantees that any reasonable numerical optimization procedure will find the point of global maximum. It turns out that the choice of good initial points for iterative optimization procedures is crucial for solution of (3.1). In the context of circle fitting with other algorithms a similar remark appears, e.g., in Kanatani & Rangarajan (2011) and Beck & Pan (2012).

The next small experiment demonstrates crucial importance of initial points selection for numerical solution of the optimization problem in (3.1). In the reduced circular structural model Anderson (1981) suggested the following intuitive initializations for parameters a, b, ρ, and σ^2:

$$\begin{gathered} a_0 = \bar{X} = \frac{1}{n}\sum_{i=1}^{n} X_i, \quad b_0 = \bar{Y} = \frac{1}{n}\sum_{i=1}^{n} Y_i, \\ \sigma_0^2 = \frac{1}{2n}\sum_{i=1}^{n}[(X_i - \bar{X})^2 + (Y_i - \bar{Y})^2 - \rho_0^2], \quad \rho_0 = \frac{1}{n}\sum_{i=1}^{n}\sqrt{(X_i - \bar{X})^2 + (Y_i - \bar{Y})^2}. \end{gathered} \tag{3.9}$$

In the full circular structural model there is no natural initialization for parameters μ and $\varkappa$ of the von Mises distribution. Therefore we draw the initial values for μ and $\varkappa$ randomly from uniform distributions on $[0, 2\pi)$ and $[0, 100]$ respectively. For 1000 replications we generate a sample of size 5000 according to (2.1)-(2.2) with $a = b = 0$, $\rho = 35$, $\sigma^2 = 4$, $\mu = 0.35\pi$ and $\varkappa = 45$. Then we solve (3.1) numerically using the interior-point algorithm implemented in `fmincon` function of the Matlab Optimization Toolbox. The initial points for the optimization procedure are chosen as described above. Figure 2 shows that approximately in 50% of the simulation runs the optimization process fails to estimate the values of a, b and ρ properly.

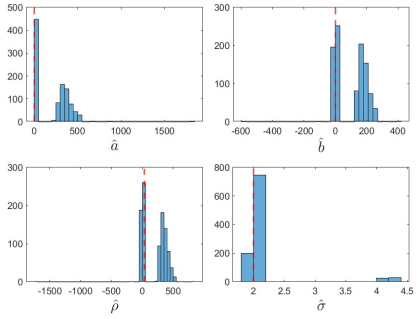

Figure 2: *Histograms of the ML estimates of a, b, ρ and σ from 1000 runs, where the true values $\theta = (0, 0, 35, 4, 0.35\pi, 45)$ are indicated by red dashed lines.*

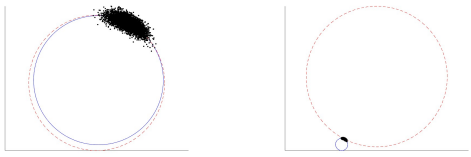

(a) **(b)**

Figure 3: *Two circle fits for the same data set when the only change is in the initial values $\mu_0, \varkappa_0$. In panel (a) the estimated circle (red dashed line) is close to the true one (blue line). In panel (b) the numerical optimization algorithm diverges.*

In addition, Figure 3 displays the results of circle fits obtained on the same data set when the same initializations for a, b, ρ, σ^2 are used with the only difference in the random initial values of μ_0, $\varkappa_0$. We observe that panel (a) of Figure 3 shows a good fit, while in panel (b) the optimization process results in a poor circle estimate. Since the simulation runs differ only in the initial values for parameters $\varkappa$

and μ, this clearly demonstrates high sensitivity of the optimization process to initial values. It is worth mentioning that the same phenomenon holds for other choices of parameters.

In view of the presented results, the need for "good" initial points in order to obtain a stable circle fitting algorithm is clear. In the next section we develop method of moments estimators which can serve as initial points for the numerical optimization in (3.1). As we show below, the use of auxiliary method of moments estimators substantially improves stability of the proposed circle fitting algorithm.

4 Method of moments

In this section we develop the method of moments estimators for $\theta := (a, b, \rho, \sigma^2, \mu, \varkappa)$. It is remarkable that the mean direction parameter μ can be estimated separately of all other parameters. The proposed estimator of μ is intimately related to the principal component analysis (PCA) of the data from the circular structural model.

4.1 PCA of circular structural model

It will be convenient to rewrite the model (2.1)-(2.2) in the following form

$$Z = m + \rho e_\varphi + \varepsilon, \tag{4.1}$$

where

$$Z := \begin{bmatrix} X \\ Y \end{bmatrix}, \quad m := \begin{bmatrix} a \\ b \end{bmatrix}, \quad e_\varphi := \begin{bmatrix} \cos\varphi \\ \sin\varphi \end{bmatrix}.$$

The next statement establishes expressions for the covariance matrix $\Sigma := \mathrm{cov}_\theta(Z)$ of the observations, and characterizes the mean direction parameter μ in terms of the spectral decomposition of Σ.

Proposition 4.1 (a). *The covariance matrix of Z, is given by*

$$\Sigma = \frac{1}{2}\begin{bmatrix} \rho^2(1 - R_1^2 + (R_2 - R_1^2)\cos 2\mu) + 2\sigma^2 & \rho^2(R_2 - R_1^2)\sin 2\mu \\ \rho^2(R_2 - R_1^2)\sin 2\mu & \rho^2(1 - R_1^2 - (R_2 - R_1^2)\cos 2\mu) + 2\sigma^2 \end{bmatrix} \tag{4.2}$$

where R_i stands for $R_i(\varkappa)$, $i = 1, 2$.

(b). *The eigenvalues of Σ are given by*

$$\begin{aligned} \lambda_{\min}(\Sigma) &= \tfrac{1}{2}\rho^2\left(1 - 2R_1^2(\varkappa) + R_2(\varkappa)\right) + \sigma^2 \\ \lambda_{\max}(\Sigma) &= \tfrac{1}{2}\rho^2\left(1 - R_2(\varkappa)\right) + \sigma^2. \end{aligned}$$

(c). *The vector e_μ associated with the mean direction parameter $\mu \in [0, 2\pi)$ is the eigenvector of matrix $\Sigma = \mathrm{cov}_\theta(Z)$ corresponding to the minimal eigenvalue $\lambda_{\min}(\Sigma)$, i.e.*

$$e_\mu = \arg\min_{\zeta \in [0, 2\pi)} e_\zeta^T \Sigma e_\zeta = \arg\min_{e_\zeta : \|e_\zeta\| = 1} e_\zeta^T \Sigma e_\zeta.$$

Several remarks on the results of Proposition 4.1 are in order. First, Proposition 4.1 shows that the vector e_μ associated with the mean direction parameter μ is the eigenvector of Σ corresponding to the smallest eigenvalue. Thus, e_μ is the second principal direction, while $e_{\mu - \pi/2}$ is the first principal direction. Second, if $\varkappa = 0$ then $\lambda_{\min}(\Sigma) = \lambda_{\max}(\Sigma) = \frac{1}{2}\rho^2 + \sigma^2$ because $R_k(0) = 0$ for all $k = 1, 2, \ldots$. This is the case of the reduced circular structural model where the mean direction is not identifiable. The similar situation holds in asymptotics as $\varkappa \to \infty$: both eigenvalues of Σ tend to σ^2, and in this case the entire model tends to be unidentifiable because the von Mises distribution degenerates to a point mass.

4.2 Estimation of mean direction

Using the property proved in part (c) of Proposition 4.1 we can easily develop an estimator of the mean direction μ as follows. Let $\hat{\Sigma}$ be the empirical covariance matrix, given by

$$\hat{\Sigma} = \frac{1}{n}\sum_{i=1}^{n}(Z_i - \bar{Z})(Z_i - \bar{Z})^T,$$

where $\bar{Z} = \frac{1}{n}\sum_{i=1}^{n} Z_i$. Then, the estimator $\hat{\mu}$ is defined by

$$\hat{\mu} = \arg\min_{\zeta\in[0,2\pi)} e_\zeta^T \hat{\Sigma} e_\zeta = \arg\min_{\zeta\in[0,2\pi)} e_\zeta^T \Big[\frac{1}{n}\sum_{i=1}^{n}(Z_i - \bar{Z})(Z_i - \bar{Z})^T\Big] e_\zeta.$$

The eigenvectors are determined up to a sign; therefore the solution is not unique, and we have two possible estimators $\hat{\mu}$, and $\hat{\mu} + \pi$ of mean direction μ. In particular, two possible solutions are given by

$$\begin{aligned}\hat{\mu}^{(1)} &= \arctan\Big(\frac{e_{\hat{\mu},2}}{e_{\hat{\mu},1}}\Big) \mod 2\pi,\\ \hat{\mu}^{(2)} &= (\hat{\mu}^{(1)} + \pi) \mod 2\pi,\end{aligned}$$

where $e_{\hat{\mu},i},\ i = 1, 2$ stands for the ith element of the empirical eigenvector corresponding to the minimal eigenvalue. Note, however, that if we restrict the mean direction parameter to belong, e.g., to $[0, \pi)$ then the solution is unique. Under these circumstances using standard methods one can establish consistency and asymptotic normality of the developed mean direction estimator.

4.3 Estimation of other model parameters

Having two possible estimates $\hat{\mu}$ of the mean direction, we proceed with development of estimators of the other model parameters a, b, ρ, $\varkappa$ and σ^2. For this purpose we derive estimating equations based on the moments of X and Y and other functionals of the joint distribution of (X, Y).

Because $\mathbb{E}_\theta \cos\varphi = R_1(\varkappa)\cos\mu$ and $\mathbb{E}_\theta \sin\varphi = R_1(\varkappa)\sin\mu$ [see (A.6) and (A.7) in Appendix A] we have that

$$\mathbb{E}_\theta(X) = a + \rho R_1(\varkappa)\cos\mu, \tag{4.7}$$
$$\mathbb{E}_\theta(Y) = b + \rho R_1(\varkappa)\sin\mu. \tag{4.8}$$

Furthermore, (4.2) implies that

$$\mathrm{var}_\theta(X) + \mathrm{var}_\theta(Y) = \rho^2(1 - R_1^2(\varkappa)) + 2\sigma^2, \tag{4.9}$$

and it follows from (4.3)-(4.4) that

$$\lambda := \lambda_{\max}(\Sigma) - \lambda_{\min}(\Sigma) = \rho^2(R_1^2(\varkappa) - R_2(\varkappa)). \tag{4.10}$$

The fifth equation is based on the formula for the moment generating function of a generic observation (X, Y). In the proof of Propostion 2.1 given in Appendix B we show that for all t_1, t_2

$$\begin{aligned}&\Psi_\theta(t_1, t_2) = \mathbb{E}_\theta e^{t_1 X + t_2 Y}\\ &= \exp\Big\{a t_1 + b t_2 + \tfrac{1}{2}\sigma^2(t_1^2 + t_2^2)\Big\}\frac{1}{I_0(\varkappa)} I_0\Big(\sqrt{(\rho t_1 + \varkappa\cos\mu)^2 + (\rho t_2 + \varkappa\sin\mu)^2}\Big).\end{aligned}$$

Therefore letting $t_1 = \cos\mu,\ t_2 = \sin\mu$ we obtain

$$\mathbb{E}_\theta\big[\exp\big\{(X - \mathbb{E}_\theta(X))\cos\mu + (Y - \mathbb{E}_\theta(Y))\sin\mu\big\}\big] = \exp\Big\{\frac{\sigma^2}{2} - \rho R_1(\varkappa)\Big\}\frac{I_0(\rho + \varkappa)}{I_0(\varkappa)}. \tag{4.11}$$

Observe that the left hand sides of equations (4.7), (4.8), (4.9), (4.10) and (4.11) can be estimated from the data, so that we have five relationships that can serve as a basis for estimating equations.

The estimating equations are obtained from the above relationships as follows. Denote S_{xx}, S_{xy} and S_{yy} the empirical estimators of $\mathrm{var}_\theta(X)$, $\mathrm{cov}_\theta(X,Y)$ and $\mathrm{var}_\theta(Y)$ respectively:

$$S_{xx} := \frac{1}{n}\sum_{i=1}^{n}(X_i - \bar{X})^2,\ S_{yy} := \frac{1}{n}\sum_{i=1}^{n}(Y_i - \bar{Y})^2,\ \ S_{xy} := \frac{1}{n}\sum_{i=1}^{n}(X_i - \bar{X})(Y_i - \bar{Y}), \tag{4.12}$$

where $\bar{X} = \frac{1}{n}\sum_{i=1}^{n} X_i$ and $\bar{Y} = \frac{1}{n}\sum_{i=1}^{n} Y_i$. From equations (4.7)-(4.8) we get

$$\begin{aligned} \hat{a} &= \bar{X} - \hat{\rho} R_1(\hat{\varkappa}) \cos\hat{\mu}, \\ \hat{b} &= \bar{Y} - \hat{\rho} R_1(\hat{\varkappa}) \sin\hat{\mu}, \end{aligned} \tag{4.13}$$

and from (4.10) we have

$$\hat{\rho} = \sqrt{\frac{\hat{\lambda}}{R_1^2(\hat{\varkappa}) - R_2(\hat{\varkappa})}}. \tag{4.14}$$

Expressing (4.9) in terms of σ^2 and plugging in $\hat{\rho}^2$, yields the equation

$$\hat{\sigma}^2 = \frac{1}{2}\left(S_{xx} + S_{yy} - \frac{1 - R_1^2(\hat{\varkappa})}{R_1^2(\hat{\varkappa}) - R_2(\hat{\varkappa})} \cdot \hat{\lambda}\right). \tag{4.15}$$

Substituting (4.13)-(4.15) and $\hat{\mu}$ in (4.11) we construct the last estimating equation:

$$\frac{1}{n}\sum_{i=1}^{n} \exp\{(X_i - \bar{X})\cos\hat{\mu} + (Y_i - \bar{Y})\sin\hat{\mu}\} = \exp\left\{\frac{\hat{\sigma}^2}{2} - \hat{\rho} R_1(\hat{\varkappa})\right\} \frac{I_0(\hat{\rho} + \hat{\varkappa})}{I_0(\hat{\varkappa})}. \tag{4.16}$$

Solution of equations (4.13)–(4.16) with respect to $\hat{a}, \hat{b}, \hat{\rho}, \hat{\sigma}^2$ and $\hat{\varkappa}$ proceeds as follows. First, by substituting equations (4.14) and (4.15) in (4.16), we obtain a single equation with respect to $\hat{\varkappa}$ only. This equation is solved numerically. Then $\hat{a}, \hat{b}, \hat{\rho}$ and $\hat{\sigma}^2$ are found by substitution in equations (4.13)–(4.15). Details on numerical solution of (4.16) are provided below in Section 6.

As discussed in Section 4.2, the estimator of the mean direction $\hat{\mu}$ is not unique; therefore we solve equation (4.16) twice and obtain two sets of the method of moments estimators corrsponding to $\mu^{(1)}$ and $\mu^{(2)}$.

It is worth noting that estimating equations (4.13)–(4.16) are valid only under the assumption that $\varkappa > 0$, i.e., the angle distribution is non–uniform. The numerical algorithm solving (4.16) becomes unstable for small values of $\varkappa$. Therefore in the implementation of the circle fitting algorithm we need to distinguish between the cases of the uniform and non–uniform angle distribution. This fact motivates the development of a test for uniformity the circular structural model. The test for uniformity in the circular structural model is of independent interest; it can be used independently of any circle fitting procedure.

5 Testing uniformity

We consider the following testing problem: test

$$H_0 : \varkappa = 0 \quad \text{versus} \quad H_1 : \varkappa > 0$$

on the basis of observations $\{(X_i, Y_i), i = 1, \ldots\}$ generated by the model (2.1)–(2.2).

Note that both the null and alternative hypotheses are composite: under the null hypothesis the vector of unknown parameters $\theta = (a, b, \rho, \sigma^2, \mu, \varkappa)$ reduces to $\theta_0 = (a, b, \rho, \sigma^2)$. The formulated testing problem has an intereting feature. Under the null hypoheses the distribution of the observations do not depend on the mean direction μ which is a nuisance parameter in this setting. As it was pointed out in Davies (1977), in such situations the generalized likelihood ratio tests are not directly applicable, and the standard chi–squared approximation of the logarithm of the likelihood ratio does not hold.

We base the proposed testing procedure on the following simple observation. It follows from statement (b) of Proposition 4.1 that under the null hypothesis H_0 the eigenvalues of the covariance matrix

Σ coincide, i.e., $\lambda_{\min}(\Sigma) = \lambda_{\max}(\Sigma)$. It is easily verified that the eigenvalues of the empirical covariance matrix $\hat{\Sigma}$ are

$$\hat{\lambda}_{1,2} = \frac{1}{2}\left(S_{xx} + S_{yy} \pm \sqrt{(S_{xx} - S_{yy})^2 + 4S_{xy}^2}\right),$$

where S_{xx}, S_{yy} and S_{xy} are given in (4.12). Define

$$\widehat{T}_n := (S_{xx} - S_{yy})^2 + 4S_{xy}^2.$$

Under the null hypothesis $\hat{T}_n$ should be close to zero, and H_0 should be rejected for large values of $\widehat{T}_n$. The next statement derives asymptotic distribution of $\widehat{T}_n$ under the null hypothesis.

Theorem 5.1 (a). *Under H_0 one has*

$$\sqrt{n}\begin{bmatrix} S_{xx} - S_{yy} \\ 2S_{xy} \end{bmatrix} \xrightarrow{d} \mathcal{N}_2(0, sI), \quad n \to \infty,$$

where $s := \frac{1}{2}\rho^4 + 4\sigma^2\rho^2 + 4\sigma^4$, and I is the identity matrix.

(b). *In addition, if*

$$\widehat{M}_n := \frac{1}{2n}\sum_{i=1}^{n}\left\{(X_i - \bar{X})^2 + (Y_i - \bar{Y})^2\right\}^2$$

then under H_0

$$\frac{n\widehat{T}_n}{\widehat{M}_n} = n\left(\frac{(S_{xx} - S_{yy})^2 + 4S_{xy}^2}{\widehat{M}_n}\right) \xrightarrow{d} \chi_2^2, \quad n \to \infty,$$

where χ_2^2 is the chi–square distribution with two degrees of freedom.

Using the results of Theorem 5.1 we propose the following test for uniformity:

reject the null hypothesis if

$$\frac{n\widehat{T}_n}{\widehat{M}_n} = n\left(\frac{(S_{xx} - S_{yy})^2 + 4S_{xy}^2}{\widehat{M}_n}\right) > \chi_{2,1-\alpha}^2,$$

where $\chi_{2,1-\alpha}^2$ is the $(1-\alpha)$–quantile of the chi-square distribution with two degrees of freedom.

According to Theorem 5.1 the significance level of the proposed test is equal to α asymptotically. The test we have developed for the hypotheses $H_0 : \varkappa = 0$ versus $H_1 : \varkappa > 0$ is based on testing equality of eigenvalues of the covariance matrix of the random vector (X, Y). In fact, the proposed procedure tests $H_0 : T = 0$ versus $H_1 : T > 0$ where

$$T := (\mathrm{var}_\theta(X) - \mathrm{var}_\theta(Y))^2 + 4\left(\mathrm{cov}_\theta(X, Y)\right)^2 = \rho^4(R_2(\varkappa) - R_1(\varkappa))^2.$$

It is clear that $T = 0$ whenever $\varkappa = 0$, but we also have $T \to 0$ as $\varkappa \to \infty$. Therefore, we expect that the test will have small power for very large values of $\varkappa$. However, it is worth mentioning that in the case of large $\varkappa$ accuracy of any statistical procedure will be poor because the model becomes non–identifiable as $\varkappa$ approaches infinity.

6 Circle fitting algorithm and simulation study

Now we are in a position to describe the proposed circle fitting algorithm. In general, the algorithm proceeds in two stages. First, we obtain auxiliary method of moments estimates of the circle parameters. On the second stage these auxiliary estimates serve as starting points for numerical maximization of the log–likelihood function. In this section we also present results of an extensive simulation study.

6.1 Implementation

The method of moments equations are given in (4.13)–(4.16). Some useful bounds on the parameter estimates can be derived from properties of the modified Bessel functions of the first kind. These bounds restrict search regions for numerical solution of moment equations and log–likelihood maximization problem, and improve stability of the proposed circle fitting algorithm.

Bounds on search region for $\hat{\varkappa}$, $\hat{\sigma}^2$ and $\hat{\mu}$. In view of (A.5) in Appendix A, $R_1^2(x) - R_2(x) \geq 0$ for all $x \geq 0$. Because $\hat{\lambda} \geq 0$, we have that

$$\frac{(1 - R_1^2(\hat{\varkappa}))\hat{\lambda}}{R_1^2(\hat{\varkappa}) - R_2(\hat{\varkappa})} \geq 0.$$

This leads to the inequality

$$\hat{\sigma}^2 = \frac{1}{2}\left(S_{xx} + S_{yy} - \frac{1 - R_1^2(\hat{\varkappa})}{R_1^2(\hat{\varkappa}) - R_2(\hat{\varkappa})} \cdot \hat{\lambda}\right) \leq \tfrac{1}{2}\left(S_{xx} + S_{yy}\right),$$

which provides an upper bound for $\hat{\sigma}^2$, in addition to the obvious lower bound of non-negativity. If $\hat{\sigma}^2 \geq 0$ then it follows from (4.15) that

$$\frac{1 - R_1^2(\hat{\varkappa})}{R_1^2(\hat{\varkappa}) - R_2(\hat{\varkappa})} \leq \frac{1}{\hat{\lambda}}\left(S_{xx} + S_{yy}\right).$$

The function $x \mapsto (1 - R_1^2(x))/(R_1^2(x) - R_2(x))$ is monotone decreasing on the positive real line. This property is easily proved by differentiating and observing that the derivative is strictly negative whenever $x > 0$. Therefore if $\varkappa_L$ denotes the value of $\varkappa$ that solves the equation

$$\frac{1 - R_1^2(\varkappa)}{R_1^2(\varkappa) - R_2(\varkappa)} = \frac{1}{\hat{\lambda}}(S_{xx} + S_{yy}), \tag{6.1}$$

then $\varkappa_L$ is a lower bound for $\hat{\varkappa}$. We remark that equation (6.1) is solved easily using the bisection method. As for the upper bound on $\hat{\varkappa}$, we note that numerical evaluation of Bessel functions fails for large values of the argument. Therefore in all our simulations we impose the upper bound of $\hat{\varkappa} \leq 500$.

Additional bounds can be derived on the mean direction $\hat{\mu}$. From (4.2) we have that $\mathrm{cov}_\theta(X, Y) = \frac{1}{2}(R_2(\varkappa) - R_1^2(\varkappa))\sin(2\mu)$. Since $R_2(x) - R_1^2(x) \leq 0$ for all $x \geq 0$, the covariance sign is determined by the sign of $\sin(2\mu)$. For negative values of $\mathrm{cov}_\theta(X, Y)$, $\sin(2\mu)$ is positive; hence $\mu \in (0, \frac{1}{2}\pi) \cup (\pi, \frac{3}{2}\pi)$. For positive covariance values, $\mu \in (\frac{1}{2}\pi, \pi) \cup (\frac{3}{2}\pi, 2\pi)$. Using these facts, we can compute S_{xy} and according to its sign we can restrict the search for $\hat{\mu}$. Specifically, each value of $\hat{\mu}^{(1)}$ and $\hat{\mu}^{(2)}$ has corresponding bounds, and we restrict the numerical algorithm to a specific quadrant.

Numerical solution of moment equations. Given lower and upper bounds on $\hat{\mu}, \hat{\varkappa}, \hat{\sigma}^2$ and estimate $\hat{\mu}$ of μ, we proceed to solve (4.13)–(4.16). First, substitution of (4.15) in (4.16) yields the equation

$$\begin{aligned} h(\hat{\varkappa}) := \exp\left\{ - \frac{\hat{\lambda}(1 - R_1^2(\hat{\varkappa}))}{4[R_1^2(\hat{\varkappa}) - R_1(\hat{\varkappa})]} - \frac{\sqrt{\hat{\lambda}}R_1(\hat{\varkappa})}{\sqrt{R_1^2(\hat{\varkappa}) - R_2(\hat{\varkappa})}}\right\} \frac{I_0\left(\hat{\varkappa} + \sqrt{\hat{\lambda}/(R_1^2(\hat{\varkappa}) - R_2(\hat{\varkappa}))}\right)}{I_0(\hat{\varkappa})} \\ = \exp\left\{ - \tfrac{1}{4}(S_{xx} + S_{yy})\right\} \cdot \frac{1}{n}\sum_{i=1}^{n} \exp\left\{(X_i - \bar{X})\cos\hat{\mu} + (Y_i - \bar{Y})\sin\hat{\mu}\right\}. \end{aligned} \tag{6.2}$$

We recall that $\hat{\rho} = \sqrt{\hat{\lambda}/(R_1^2(\hat{\varkappa}) - R_2(\hat{\varkappa}))}$. The right hand side of (6.2) is a statistic, and the equation should be soved with respect to $\hat{\varkappa}$. Although function $h(\hat{\varkappa})$ on the left hand side of (6.2) depends on $\hat{\varkappa}$ in a rather complicated way, the equation (6.2) can be solved efficiently. This is equation of the type $h(x) = \mathrm{const}$, and Figure 4 displays function $h(x)$ for different values of $\hat{\lambda}$. We solve (6.2) on the interval $[\varkappa_L, 500]$ using the trust region reflective algorithm, implemented in the function `lsqnonlin` of the Matlab Optimization Toolbox. The stopping criteria *MaxFunctionEvaluations, OptimalityTolerance* and *StepTolerance* were modified to 1e10, 1e−20 and 1e−20 respectively to account for flatness of function h for large values of the argument. Given estimates of $\varkappa$ and μ, we plug them in (4.13)-(4.15) and obtain the moment estimators of a, b, ρ, and σ^2.

Numerical solution of the likelihood maximization problem. Depending on the results of the uniformity test, the ML estimator is constructed by solution of the optimization problem for the full

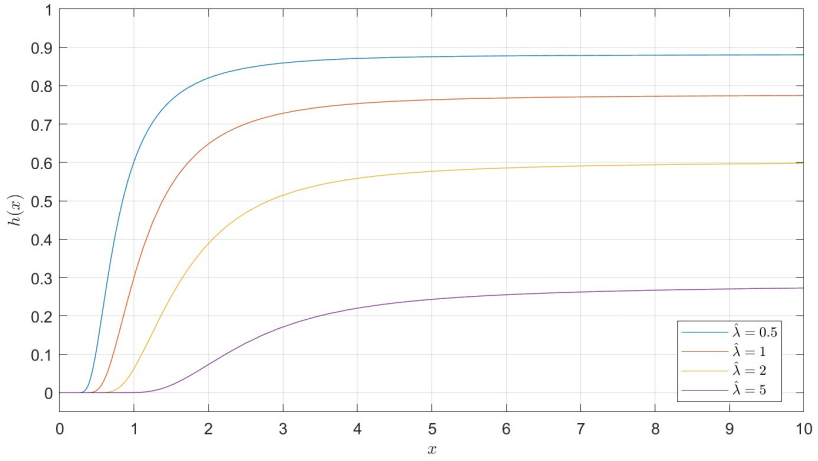

Figure 4: *Function $h(x)$ in (6.2) for different values of $\hat{\lambda}$.*

or reduced circular structural model. In both cases we use the interior-point algorithm implemented in `fmincon` function of the Matlab Optimization Toolbox with default stopping criteria. For the full circular model the initial points are the auxiliary moment estimators obtained as described above. For the reduced circular structural model we use the initial points (3.9) as proposed in Anderson (1981). Another remark concerns with the method of moments estimate $\hat{\sigma}^2$ as a starting point for the numerical likelihood maximization. Our experience shows that whenever $\hat{\sigma}^2$ is too close to zero (the boundary of parameter space), the numerical likelihood maximization with such initial points often diverges. To prevent the divergence, as an initial point for σ^2 we select the method of moments estimate $\hat{\sigma}^2$ perturbed by addition of an exponential random variable with expectation equal to one.

Circle fitting algorithm. The proposed circle fitting algorithm includes the following steps.

1. Perform the test of uniformity described in Section 5. For our implementation we use $\alpha = 0.05$.
2. If the test does not reject the null hypothesis H_0, then set $\hat{\varkappa} = 0$ and proceed with estimating $\theta_0 = (a, b, \rho, \sigma^2)$ in the reduced circular structural model as described in Anderson (1981). The corresponding optimization problem is given in (3.2). The initial points for the numerical procedure are chosen according to (3.9).
3. If the test rejects the null hypothesis then perform the following steps.
   (i). Compute the estimate of the mean direction $\hat{\mu}$ as described in Section 4.2 and obtain two potential values $\hat{\mu}^{(1)}$ and $\hat{\mu}^{(2)}$.
   (ii). For $\hat{\mu}^{(i)}$, $i = 1, 2$ solve the method of moments equations (4.13)–(4.16) and find two sets of moments estimates for θ.
   (iii). Solve the optimization problem in (3.1) twice, each time for different set of initial points given by the moment estimators of step (ii).
   (iv). Among the two solutions obtained in the step (iii) above, choose the one having higher log–likelihood value. This is the sought maximum likelihood estimate and the algorithm output.

The Matlab code implementing the above circle fitting algorithm along with documentation can be found on the Github repository.

6.2 Simulation experiments

The goal of the following simulation study is to assess accuracy of the proposed algorithm under different combinations of model parameters, to study its sensitivity to distributional assumptions and to compare

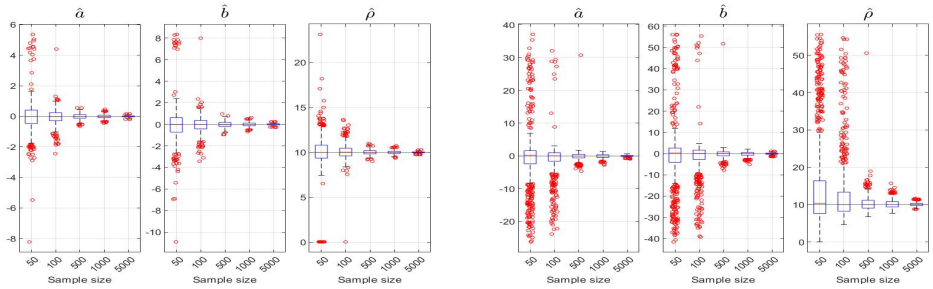

(a) $\varkappa = 5,\ \mu = \pi/3$ **(b)** $\varkappa = 20,\ \mu = \pi/3$

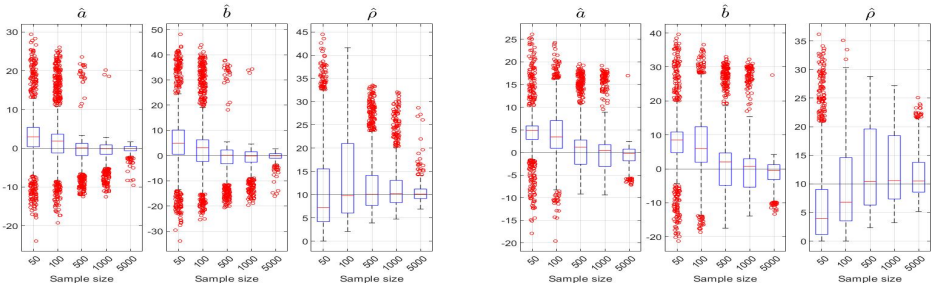

(c) $\varkappa = 50,\ \mu = \pi/3$ **(d)** $\varkappa = 80,\ \mu = \pi/3$

Figure 5: *Simulation results for* $a = b = 0,\ \rho = 10$ *and* $\sigma = 1$.

it with commonly used circle fitting algorithms. The following experiments have been performed in our simulation study.

1. Experiment 1: we assess performance of the algorithm for different combinations of values of $\rho, \sigma^2, \varkappa$ and sample sizes n. The data are generated from the circular structural model with the von-Mises angle distribution.

2. Experiment 2: we compare our algorithm with the Levenberg-Marquardt algorithm (LM), the Pratt and Taubin fits for different combinations of parameter values.

3. Experiment 3: we study sensitivity of our algorithm to misspecification of angle distribution; the angles are generated from the uniform and beta distributions.

Experiment 1. First we consider the simulation setup reported in Anderson (1981) and Chan (1965); here $a = b = 0, \rho = 10, \sigma = 1$. In addition, we fix $\mu = \pi/3$. Figure 5 presents boxplots of the obtained estimators for increasing sample sizes, where each panel is based on different value of $\varkappa = 5, 20, 50, 80$. The black solid lines indicate the true values of parameters. We can see that larger values of concentration parameter $\varkappa$ resulted in higher variability of the proposed fit. The graphs demonstrate that estimation accuracy improves with the sample size.

Figure 6 displays the results for the same values of $\varkappa$ and μ but with larger radius $\rho = 20$. In comparison with Figure 5 we observe some improvement in the estimator performance in terms of bias, but still the resulted variance is quite large. Note that the results in Figures 5 and 6 correspond to the high–noise scenario; here the noise standard deviation is $\sigma = 1$

The situation is completely different in the small–noise scenario. The setting with $\sigma = 0.05$ and $\rho = 1$ appears frequently in the literature on circle fitting [see, e.g., Berman (1989), Al-Sharadqah & Chernov (2009)]. Figure 7 presents the results, and we observe that the variance reduced dramatically compared to the case where $\rho = 20$, $\sigma = 1$, even though the ratio ρ/σ is the same as in the setting of Figure 6.

Experiment 2 In this experiment we compare our algorithm with three state–of–the–art circle fitting algorithms. The Levenberg-Marquardt fit is a general purpose non–linear least squares optimization algorithm applied to the geometric fit optimization problem (1.2). The Pratt and Taubin fits solve

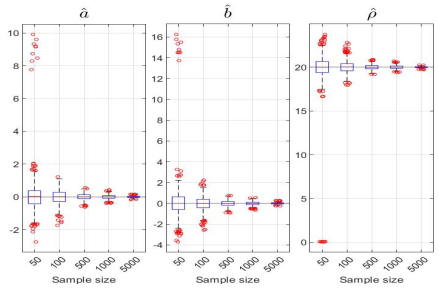

(a) $\varkappa = 5,\ \mu = \pi/3$

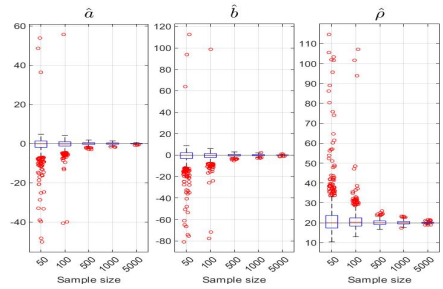

(b) $\varkappa = 20,\ \mu = \pi/3$

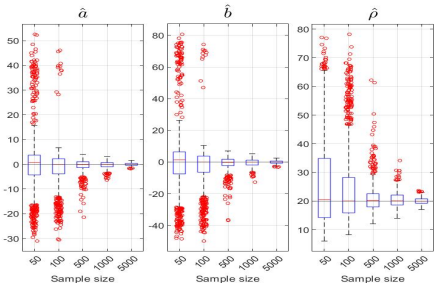

(c) $\varkappa = 50,\ \mu = \pi/3$

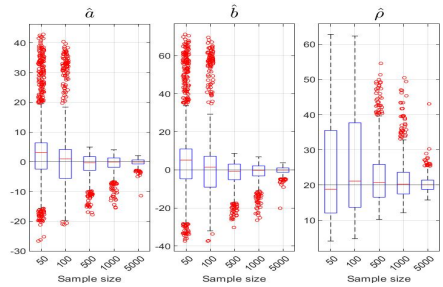

(d) $\varkappa = 80,\ \mu = \pi/3$

Figure 6: *Simulation results for* $a = b = 0,\ \rho = 20$ *and* $\sigma = 1$.

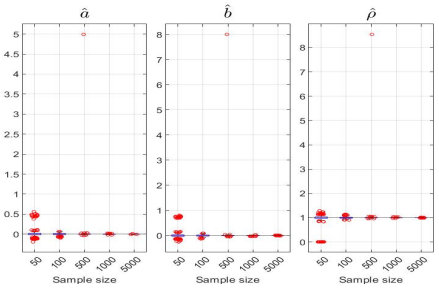

(a) $\varkappa = 5,\ \mu = \pi/3$

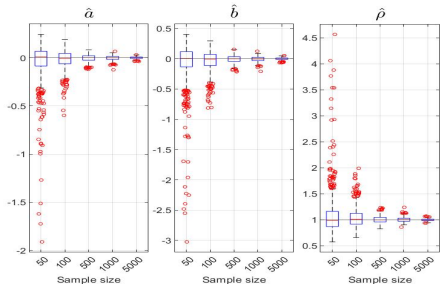

(b) $\varkappa = 20,\ \mu = \pi/3$

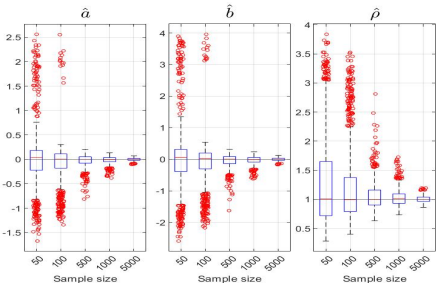

(c) $\varkappa = 50,\ \mu = \pi/3$

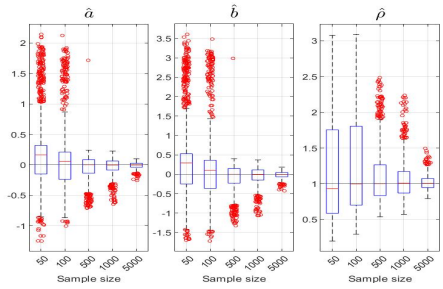

(d) $\varkappa = 80,\ \mu = \pi/3$

Figure 7: *Simulation results for* $a = b = 0,\ \rho = 1$ *and* $\sigma = 0.05$.

optimization problems of the algebraic fit type with algebraic parametrization of the circle equation.

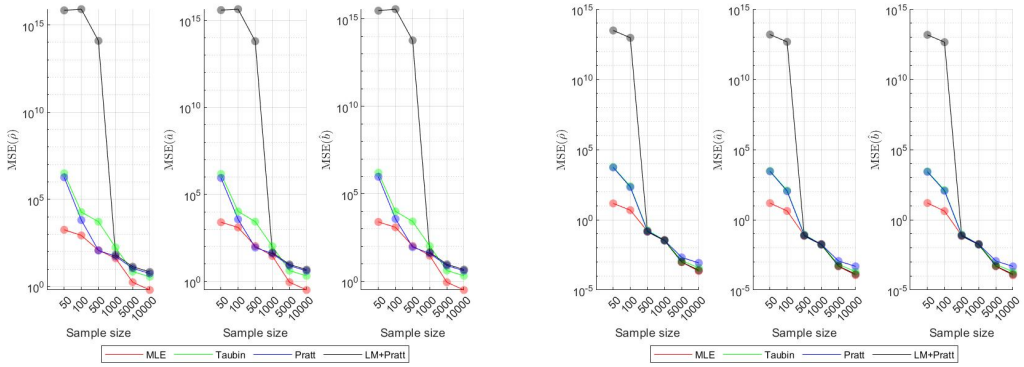

(a) $a = b = 0, \rho = 10, \sigma = 1$ and $\varkappa = 60$ **(b)** $a = b = 0, \rho = 1, \sigma = 0.05$ and $\varkappa = 60$

Figure 8: *MSE on logarithmic scale for different algorithms when* $\varphi_i \sim \mathrm{vM}(\frac{\pi}{4}, \varkappa)$.

In particular, the Pratt fit solves the following optimization problem

$$\begin{aligned} \min_{A,B,C,D} \quad & \sum_{i=1}^{n} \left(A(X_i^2 + Y_i^2) + BX_i + CY_i + D\right)^2 \\ \text{s.t.} \quad & B^2 + C^2 - 4AD = 1, \end{aligned}$$

while the Taubin fit is a solution to

$$\begin{aligned} \min_{A,B,C,D} \quad & \sum_{i=1}^{n} \left(A(X_i^2 + Y_i^2) + BX_i + CY_i + D\right)^2, \\ \text{s.t.} \quad & 4A^2(\overline{X^2} + \overline{Y^2}) + 4AB\bar{X} + 4AC\bar{Y} + B^2 + C^2 = 1, \end{aligned}$$

where $\overline{X^2} = \frac{1}{n}\sum_{i=1}^{n} X_i^2$, and $\overline{Y^2} = \frac{1}{n}\sum_{i=1}^{n} Y_i^2$. Figure 8 displays mean squared errors of different methods in estimating the circle center and radius when the angles follow the von Mises distribution with indicated parameters. We observe that the ML estimator proposed in this paper is superior. In addition, for larger values of σ, the ML estimator shows even better performance in comparison with the other circle fitting algorithms.

Experiment 3 Now we consider the same settings as in Experiment 2 but with a different angle distribution so that the distributional assumptions of the ML estimator do not hold. First, we set $\varphi_i \sim U(0, \pi/4)$. Figure 9 presents the results in the small–noise regime with $\sigma = 0.05$. We observe that the proposed estimator still shows good performance but not as good as the other circle fitting algorithms. For larger measurement error variance σ^2, the differences between the mean squared errors of the considered methods become smaller. However, if we consider the setting with angles generated from Beta(2,5) and Beta(1,6) distributions then even though the distributional assumptions do not hold, the ML estimator outperforms the other circle fitting algorithms. Figure 10 displays the corresponding graphs.

The simulation results presented above demonstrate that cases with high concentration of the angles (large values of $\varkappa$) are more difficult, and they result in larger bias and variance of the ML estimator. In addition, accuracy is sensitive to changes in σ^2, and the proposed estimator shows better performance in comparison to the algebraic and geometric fits, when the noise variance is larger. In terms of 'signal-to-noise' ratio ρ/σ, it is clear that larger ratio yields better performance. In addition, for fixed value of ρ/σ the variance of the ML estimator is lower when ρ and σ are smaller. Finally, the ML estimator tends to obtain good results even when the distributional assumptions on the unobservable angle variables do not hold.

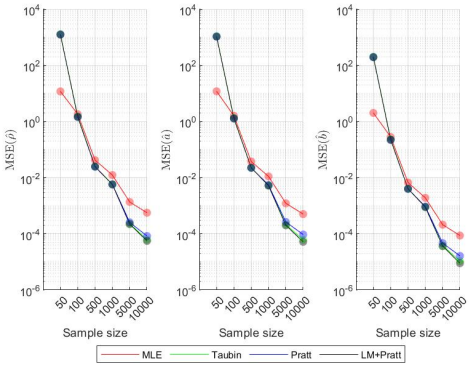

(a) $a = b = 0, \rho = 1, \sigma = 0.05$

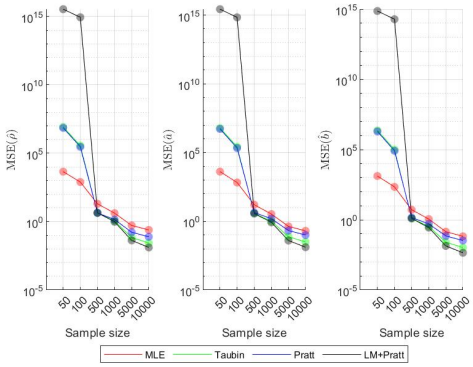

(b) $a = b = 0, \rho = 10, \sigma = 1$

Figure 9: *MSE on logarithmic scale for different algorithms when* $\varphi_i \sim U(0, \pi/4)$.

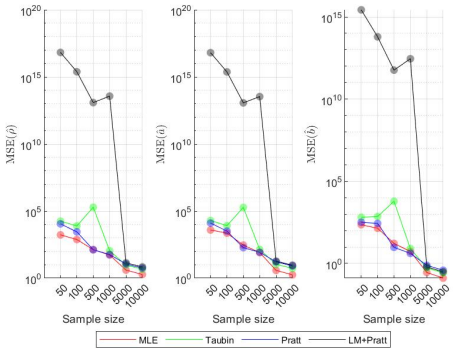

(a) MSE values on logarithmic scale for $a = b = 0, \rho = 10, \sigma = 1$

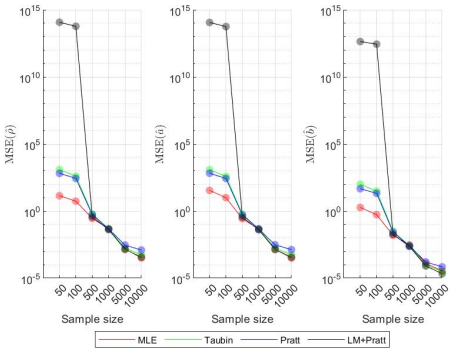

(b) MSE values on logarithmic scale for $a = b = 0, \rho = 1, \sigma = 0.05$

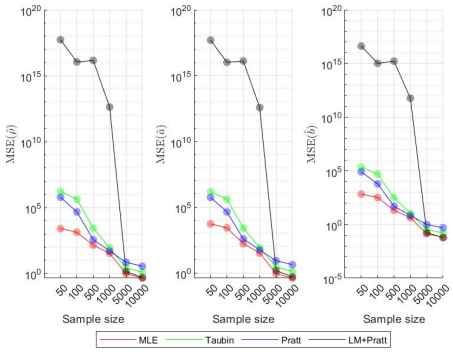

(c) MSE values on logarithmic scale for $a = b = 0, \rho = 10, \sigma = 1$

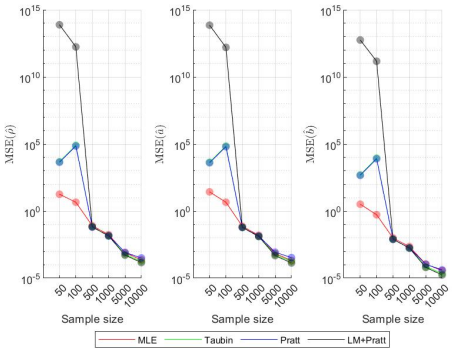

(d) MSE values on logarithmic scale for $a = b = 0, \rho = 1, \sigma = 0.05$

Figure 10: *In panels (a)-(b) the angles are generated from* Beta$(2, 5)$*, and in panels (c)-(d) from* Beta$(1, 6)$.

A Bessel functions and von Mises distribution

In this section for the ease of reference we collect well known facts about the modified Bessel functions of the first kind and the von Mises distribution. For comprehensive discussion we refer to classical books Mardia & Jupp (2000) and Watson (1944).

A.1 Modified Bessel function of first kind

The modified Bessel function $I_\nu(z)$ of the first kind of order ν is given by the infinite series

$$I_\nu(z) = (\tfrac{1}{2}z)^\nu \sum_{j=0}^{\infty} \frac{(\frac{1}{4}z^2)^j}{j!\Gamma(\nu+j+1)},$$

where $\Gamma(\cdot)$ is the Gamma function. For integer $\nu = k = 0, \pm1, \pm2, \ldots$ the following integral representation holds:

$$I_k(z) = \frac{1}{2\pi}\int_0^{2\pi} \cos(k\theta) e^{z\cos\theta}\mathrm{d}\theta, \quad z \in \mathbb{C}. \tag{A.1}$$

The following relationships involving the Bessel functions $I_k(z)$ are important for our purposes.

(i). For any $a, b \in \mathbb{R}$ one has

$$\int_0^{2\pi} e^{a\cos\theta + b\cos\theta}\mathrm{d}\theta = I_0\left(\sqrt{a^2+b^2}\right). \tag{A.2}$$

(ii). The modified Bessel function of first kind has the following property:

$$\frac{\mathrm{d}}{\mathrm{d}z} I_k(z) = I_{k+1}(z) + \frac{k}{z} I_k(z), \tag{A.3}$$

and specifically $\frac{\mathrm{d}}{\mathrm{d}z} I_0(z) = I_1(z)$.

(iii). The following recursive relationship holds:

$$I_k(z) = \frac{2(k+1)}{z} I_{k+1}(z) + I_{k+2}(z). \tag{A.4}$$

In addition, for $k \geq -1$ and real positive z on has

$$I_{k-1}(z) I_{k+1}(z) < I_k^2(z); \tag{A.5}$$

see Segura (2011). Dividing (A.5) by $I_{k-1}^2(z)$ we obtain that

$$\frac{I_{k+1}(z)}{I_{k-1}(z)} < \frac{I_k^2(z)}{I_{k-1}^2(z)}.$$

(iv). For $\nu > -0.5$ and real $z > 0$ one has $I_\nu(z) > I_{\nu+1}(z)$ [see Soni (1965)]; therefore

$$0 \leq R_{k+1}(z) \leq R_k(z) \leq 1, \quad \forall z > 0, \ \ \forall k.$$

A.2 The von Mises distribution

We repeatedly use formulas for moments of the von Mises distribution. If $\varphi \sim \mathrm{vM}(\mu, \varkappa)$, then

$$\begin{aligned}
\mathbb{E}\left(\cos(k\varphi)\right) &= \frac{1}{2\pi I_0(\varkappa)} \int_0^{2\pi} \cos(k\varphi) \cdot e^{\varkappa\cos(\varphi-\mu)}\mathrm{d}\varphi \\
&= \frac{1}{2\pi I_0(\varkappa)} \int_\mu^{2\pi+\mu} \cos(k(\alpha+\mu)) \cdot e^{\varkappa\cos\alpha}\mathrm{d}\alpha \\
&= \frac{1}{2\pi I_0(\varkappa)} \left[\int_\mu^{2\pi+\mu} \cos(k\alpha)\cos(k\mu) \cdot e^{\varkappa\cos\alpha}\mathrm{d}\alpha - \int_\mu^{2\pi+\mu} \sin(k\alpha)\sin(k\mu) \cdot e^{\varkappa\cos\alpha}\mathrm{d}\alpha\right],
\end{aligned}$$

where the second line is obtained by change of variables. By periodicity of the sine and cosine, (A.1) and the fact that

$$\int_0^{2\pi} \sin(kx) e^{\varkappa \cos x} \mathrm{d}x = 0, \quad \forall k = 0, \pm 1, \pm 2, \dots$$

we get

$$\mathbb{E}\left(\cos(k\varphi)\right) = R_k(\varkappa)\cos(k\mu), \quad \forall k = 0, \pm 1, \pm 2, \dots. \tag{A.6}$$

Similar calculation yields

$$\mathbb{E}\left(\sin(k\varphi)\right) = R_k(\varkappa)\sin(k\mu), \quad \forall k = 0, \pm 1, \pm 2, \dots. \tag{A.7}$$

Using trigonometric identities and (A.6)-(A.7) we derive the following results:

$$\mathbb{E}(\sin^2\varphi) = \mathbb{E}\left(\frac{1-\cos 2\varphi}{2}\right) = \frac{1}{2}\big(1 - R_2(\varkappa)\cos(2\mu)\big) \tag{A.8}$$

$$\mathbb{E}(\cos^2\varphi) = \mathbb{E}\left(\frac{1+\cos 2\varphi}{2}\right) = \frac{1}{2}\big(1 + R_2(\varkappa)\cos(2\mu)\big). \tag{A.9}$$

B Proofs

B.1 Proof of Proposition 2.1

First, we compute the moment generating function $\Psi_\theta(t_1, t_2) := \mathbb{E}_\theta(e^{t_1 X + t_2 Y})$ of (X, Y). By independence of $\{\varphi_i\}$, $\{\xi_i\}$ and $\{\eta_i\}$ we have

$$\begin{aligned}\Psi_\theta(t_1, t_2) &= e^{t_1 a + t_2 b} \cdot \mathbb{E}_\theta(\exp\left\{\rho(t_1\cos\varphi + t_2\sin\varphi)\right\}) \cdot \mathbb{E}_\theta(\exp\left\{t_1\xi + t_2\eta\right\}) \\ &= \exp\left\{t_1 a + t_2 b + \tfrac{1}{2}\sigma^2(t_1^2 + t_2^2)\right\} \cdot \mathbb{E}_\theta(\exp\left\{\rho(t_1\cos\varphi + t_2\sin\varphi)\right\}).\end{aligned}$$

Furthermore,

$$\begin{aligned}\mathbb{E}_\theta(\exp\left\{\rho(t_1\cos\varphi + t_2\sin\varphi)\right\}) &= \frac{1}{2\pi I_0(\varkappa)}\int_0^{2\pi} \exp\{\rho(t_1\cos\varphi + t_2\sin\varphi)\} e^{\varkappa\cos(\varphi-\mu)}\mathrm{d}\varphi \\ &= \frac{1}{2\pi I_0(\varkappa)}\int_0^{2\pi} \exp\Big\{(\rho t_1 + \varkappa\cos\mu)\cos\varphi + (\rho t_2 + \varkappa\sin\mu)\sin\varphi\Big\}\mathrm{d}\varphi \\ &= \frac{1}{I_0(\varkappa)} I_0\big(\sqrt{(\rho t_1 + \varkappa\cos\mu)^2 + (\rho t_2 + \varkappa\sin\mu)^2}\big).\end{aligned}$$

Therefore

$$\Psi_\theta(t_1, t_2) = \exp\left\{a t_1 + b t_2 + \tfrac{1}{2}\sigma^2(t_1^2 + t_2^2)\right\} \frac{1}{I_0(\varkappa)} I_0\Big(\sqrt{(\rho t_1 + \varkappa\cos\mu)^2 + (\rho t_2 + \varkappa\sin\mu)^2}\Big).$$

Let $\theta_1 = (a_1, b_1, \rho_1, \sigma_1^2, \mu_1, \varkappa_1)$, and $\theta_2 = (a_2, b_2, \rho_2, \sigma_2^2, \mu_2, \varkappa_2)$, $\theta_1, \theta_2 \in \Theta$. We will show that the equality

$$\Psi_{\theta_1}(t_1, t_2) = \Psi_{\theta_2}(t_1, t_2), \quad \forall t_1, t_2 \tag{B.1}$$

implies that $\theta_1 = \theta_2$. This fact will imply the identifiability of the model.

The moment generating function $\Psi_\theta(t_1, t_2)$ is factored to a product of two functions:

$$\begin{aligned}\Psi_\theta(t_1, t_2) &= \Psi^{(1)}_{a,b,\sigma^2}(t_1, t_2)\Psi^{(2)}_{\rho,\varkappa,\mu}(t_1, t_2) \\ &= \exp\left\{t_1 a + t_2 b + \tfrac{1}{2}\sigma^2(t_1^2 + t_2^2)\right\} \times \frac{I_0\big(\sqrt{(\rho t_1 + \varkappa\cos\mu)^2 + (\rho t_2 + \varkappa\sin\mu)^2}\big)}{I_0(\varkappa)},\end{aligned} \tag{B.2}$$

where the first one is a normal factor depending on a, b and σ^2 only, while the second one depends on ρ, $\varkappa$ and μ only.

In view of factorization (B.2), if (B.1) holds then necessarily

$$\Psi^{(1)}_{a_1,b_1,\sigma_1^2}(t_1,t_2) = \Psi^{(1)}_{a_2,b_2,\sigma_2^2}(t_1,t_2), \quad \forall t_1,t_2, \tag{B.3}$$

$$\Psi^{(2)}_{\rho_1,\varkappa_1,\mu_1}(t_1,t_2) = \Psi^{(2)}_{\rho_2,\varkappa_2,\mu_2}(t_1,t_2), \quad \forall t_1,t_2. \tag{B.4}$$

It follows from the equality of the normal factors (B.3) that

$$a_1t_1 + b_1t_2 + \tfrac{1}{2}\sigma_1^2(t_1^2+t_2^2) = a_2t_1 + b_2t_2 + \tfrac{1}{2}\sigma_2^2(t_1^2+t_2^2), \quad \forall t_1,t_2,$$

and the two polynomials are equal if and only if $a_1 = a_2$, $b_1 = b_2$ and $\sigma_1^2 = \sigma_2^2$.

Next consider equality (B.4). We have

$$\Psi^{(2)}_{\rho,\varkappa,\mu}(t_1,0) = \frac{1}{I_0(\varkappa)} I_0\Big(\sqrt{\varkappa^2 + \rho^2 t_1^2 + 2\varkappa\rho t_1\cos\mu}\Big), \quad \forall t_1$$
$$\Psi^{(2)}_{\rho,\varkappa,\mu}(0,t_2) = \frac{1}{I_0(\varkappa)} I_0\Big(\sqrt{\varkappa^2 + \rho^2 t_2^2 + 2\varkappa\rho t_2\sin\mu}\Big), \quad \forall t_2.$$

Therefore

$$\frac{\partial}{\partial t_1}\Psi^{(2)}_{\rho,\varkappa,\mu}(t_1,0)\Big|_{t_1=0} = R_1(\varkappa)\rho\cos\mu, \quad \frac{\partial}{\partial t_2}\Psi^{(2)}_{\rho,\varkappa,\mu}(0,t_2)\Big|_{t_2=0} = R_1(\varkappa)\rho\sin\mu.$$

Equating the above partial derivatives for parameters $(\rho_1,\varkappa_1,\mu_1)$ and $(\rho_2,\varkappa_2,\mu_2)$ we obtain

$$\mu_1 = \mu_2, \quad R_1(\varkappa_1)\rho_1 = R_1(\varkappa_2)\rho_2. \tag{B.5}$$

Furthermore, for given $(\rho_1,\varkappa_1,\mu)$ and $(\rho_2,\varkappa_2,\mu)$ assume for definiteness that $\cos\mu \neq 0$. Let $t_1^* = -2\varkappa_1\cos\mu/\rho_1$; then

$$\Psi^{(2)}_{\rho_1,\varkappa_1,\mu}(t_1^*,0) = 1,$$
$$\Psi^{(2)}_{\rho_2,\varkappa_2,\mu}(t_1^*,0) = \frac{1}{I_0(\varkappa_2)} I_0\Big(\sqrt{\varkappa_2^2 + 4\varkappa_1(\rho_2/\rho_1)^2\cos^2\mu - 4(\rho_2/\rho_1)\varkappa_1\varkappa_2\cos^2\mu}\Big).$$

Hence equation $\Psi^{(2)}_{\rho_1,\varkappa_1,\mu}(t_1^*,0) = \Psi^{(2)}_{\rho_2,\varkappa_2,\mu}(t_1^*,0)$ along with the monotonicity of $I_0(\cdot)$ imply that

$$\varkappa_2 = \sqrt{\varkappa_2^2 + 4\varkappa_1(\rho_2/\rho_1)^2\cos^2\mu - 4(\rho_2/\rho_1)\varkappa_1\varkappa_2\cos^2\mu},$$

which is equivalent to

$$\frac{4\varkappa_1\rho_2}{\rho_1}\cos^2\mu\Big(\frac{\rho_2}{\rho_1}\varkappa_1 - \varkappa_2\Big) = 0 \quad \Rightarrow \quad \varkappa_1\rho_2 = \varkappa_2\rho_1.$$

Combining this with (B.5) we obtain $\varkappa_1 R_1(\varkappa_1) = \varkappa_2 R_2(\varkappa_2)$. Below we show that function $x \mapsto xR_1(x)$ is monotone increasing on the positive real line. Therefore equality $\varkappa_1 R_1(\varkappa_1) = \varkappa_2 R_2(\varkappa_2)$ implies that $\varkappa_1 = \varkappa_2$ and hence $\rho_1 = \rho_2$. This proves the identifiability under assumption that $\cos\mu \neq 0$. If $\cos\mu = 0$ then we let $t_2^* = -2\varkappa_2\sin\mu/\rho_2$ and consider the equation $\Psi^{(2)}_{\rho_1,\varkappa_1,\mu}(0,t_2^*) = \Psi^{(2)}_{\rho_2,\varkappa_2,\mu}(0,t_2^*)$. Then the same reasoning as above yields the result.

It remains to show that function $x \mapsto xR_1(x)$ is monotone increasing. We have

$$\begin{aligned}\frac{\mathrm{d}}{\mathrm{d}x}[xR_1(x)] &= \frac{I_1(x)}{I_0(x)} + x\frac{I_1'(x)}{I_0(x)} - x\left(\frac{I_1(x)}{I_0(x)}\right)^2 = \frac{I_1(x)}{I_0(x)} + x\frac{I_2(x)+\frac{1}{x}I_1(x)}{I_0(x)} - x\left(\frac{I_1(x)}{I_0(x)}\right)^2 \\ &= \frac{2I_1(x)}{I_0(x)} + \frac{x}{I_0(x)}\left(I_0(x) - \frac{2}{x}I_1(x)\right) - x\left(\frac{I_1(x)}{I_0(x)}\right)^2 = x(1-R_1^2(x)),\end{aligned}$$

where the second equality follows from $I_1'(x) = I_2(x) + \frac{1}{x}I_1(x)$ and the third one is a consequence of $I_2(x) + \frac{2}{x}I_1(x) = I_0(x)$; see (A.3) and (A.4). Since $0 \le R_1(x) \le 1$, the function $x \mapsto xR_1(x)$ is monotone increasing for positive x, as claimed. ∎

B.2 Proof of Theorem 3.1

The proof of Theorem 3.1 is based on verification of conditions of Theorem 8.1 in Chapter 1 of Ibragimov & Hasminskii (1981) for the circular structural model of Section 2. For ease of notation in the subsequent proof we write $\theta = (\theta_1, \theta_2, \theta_3, \theta_4, \theta_5, \theta_6) := (a, b, \rho, \sigma^2, \mu, \varkappa)$.

We need to verify the following conditions: there exists a number $0 < \delta \leq 1$ such that for any compact set $K \subset \Theta$ one has

$$\sup_{\theta \in K} \mathbb{E}_\theta \Big| \frac{\partial}{\partial \theta_i} \ell_1(\theta; X_1, Y_1) \Big|^{2+\delta} < \infty, \quad \forall i = 1, \ldots, 6, \tag{B.6}$$

$$\sup_{\theta \in K} \mathbb{E}_\theta \Big| \frac{\partial^2}{\partial \theta_i \partial \theta_j} \ell_1(\theta; X_1, Y_1) \Big|^{1+\delta} < \infty, \quad \forall i, j = 1, \ldots, 6, \tag{B.7}$$

$$\mathbb{E}_\theta \Big[\sup_{\theta, \theta' \in K} \Big| \frac{\partial^2}{\partial \theta_i \partial \theta_j} \ell_1(\theta; X_1, Y_1) - \frac{\partial^2}{\partial \theta_i \partial \theta_j} \ell_1(\theta'; X_1, Y_1) \Big| \cdot \|\theta - \theta'\|^{-\delta} \Big] < \infty, \quad \forall i, j = 1, \ldots, 6. \tag{B.8}$$

In fact, we will show that (B.6)–(B.8) are fulfilled with $\delta = 1$.

Verification of (B.6). Since $R_1(x)/x \leq 1$ for all x we have from (3.3) that for any positive number $m \geq 1$

$$\mathbb{E}_\theta \Big| \frac{\partial}{\partial a} \ell_1(\theta; X_1, Y_1) \Big|^m \leq \frac{2^{m-1}}{\sigma^{2m}} \big(\mathbb{E}_\theta |X_1 - a|^m + \rho^m \varkappa^m \big) < \infty.$$

Thus (B.6) is fulfilled for the random variable $\frac{\partial}{\partial a} \ell_1(\theta; X_1, Y_1)$: all moments are bounded when θ varies in a compact set. The same is true for the random variable $\frac{\partial}{\partial b} \ell_1(\theta; X_1, Y_1)$. We also have

$$\begin{aligned} \mathbb{E}_\theta \Big| \frac{\partial}{\partial \rho} \ell_1(\theta; X_1, Y_1) \Big|^m \leq \frac{2^{m-1}}{\sigma^{2m}} \Big\{ \frac{2^{m-1} \rho^m}{\sigma^{2m}} \Big(& \mathbb{E}_\theta [(X_1 - a)^2 + (Y_1 - b)^2]^m \\ & + \varkappa^m \mathbb{E}_\theta [(X_1 - a)^2 + (Y_1 - b)^2]^{m/2} \Big) + \frac{\rho^m}{\sigma^{2m}} \Big\} < \infty \end{aligned}$$

for any $\theta \in K$. The similar reasoning applies in order to establish boundedness of all moments of the remaining partial derivatives of $\ell_1(\theta; X_1, Y_1)$ in (3.6)–(3.8).

Verification of (B.7). First, we note that in view of (A.3) and (A.4) we have

$$R_k'(x) = R_{k+1}(x) + \frac{k}{x} R_k(x) - R_k(x) R_1(x),$$

and therefore

$$\frac{\mathrm{d}}{\mathrm{d}x} \Big(\frac{R_k(x)}{x} \Big) = \frac{1}{x} [R_{k+1}(x) - R_k(x) R_1(x)].$$

In particular, $\frac{\mathrm{d}}{\mathrm{d}x} \big(R_1(x)/x \big) = [R_2(x) - R_1^2(x)]/x$. Observing that

$$R_k(x) = \frac{I_k(x)}{I_0(x)} = \prod_{j=1}^k \frac{I_j(x)}{I_{j-1}(x)}$$

and using bounds on $I_j(x)/I_{j-1}(x)$ derived in Amos (1974) we have

$$\prod_{j=1}^k \Big(\frac{x}{j + \sqrt{x^2 + j^2}} \Big) \leq R_k(x) \leq \prod_{j=1}^k \Big(\frac{x}{j - 1 + \sqrt{x^2 + (j+1)^2}} \Big).$$

This inequality implies that

$$R_k(x)/x^m \leq 1, \quad \forall 0 \leq m \leq k, \tag{B.9}$$

and, in particular, $\frac{\mathrm{d}}{\mathrm{d}x} (R_k(x)/x) \leq 1$.

By (3.3)–(3.8), the first order partial derivatives of $\ell(\theta; x, y)$ with respect to θ_i, $i = 1, \dots, 6$ have the following representation

$$\frac{\partial \ell_1(\theta; x, y)}{\partial \theta_i} = \frac{R_1(D_\theta)}{D_\theta} u_i(\theta; x, y) + v_i(\theta; x, y), \quad i = 1, \dots, 6. \tag{B.10}$$

For instance, for the partial derivative with respect to $\theta_1 = a$ we have

$$u_1(\theta; x, y) = -\frac{1}{\sigma^2}(x - a) - \frac{\rho}{\sigma^2}\varkappa \cos\mu, \quad v_1(\theta; x, y) = \frac{1}{\sigma^2}(x - a),$$

while for $\theta_3 = \rho$ we have $v_3(\theta; x, y) = -\rho/\sigma^2$ and

$$u_3(\theta; x, y) = \frac{\rho}{\sigma^4}\big[(x - a)^2 + (y - b)^2\big] + \frac{\varkappa}{\sigma^2}\big[(x - a)\cos\mu + (y - b)\sin\mu\big].$$

We note that all functions $u_i(\theta; x, y)$ and $v_i(\theta; x, y)$ are infinitely differentiable with respect to θ, so that

$$\frac{\partial^2 \ell_1(\theta; x, y)}{\partial \theta_i \partial \theta_j} = \frac{\partial}{\partial \theta_j}\Big(\frac{R_1(D_\theta)}{D_\theta}\Big) u_i(\theta; x, y) + \frac{R_1(D_\theta)}{D_\theta}\frac{\partial u_i(\theta; x, y)}{\partial \theta_j} + \frac{\partial v_i(\theta; x, y)}{\partial \theta_j}. \tag{B.11}$$

Because random variables $X - a$ and $Y - b$ have finite moments of all orders we have that for any compact set $K \subset \Theta$ and $m \geq 1$

$$\sup_{\theta \in K} \mathbb{E}_\theta \left| \frac{\partial u_i(\theta; X_1, Y_1)}{\partial \theta_j} \right|^m < \infty, \quad \sup_{\theta \in K} \mathbb{E}_\theta \left| \frac{\partial v_i(\theta; X_1, Y_1)}{\partial \theta_j} \right|^m < \infty, \quad \forall i, j = 1, \dots, 6. \tag{B.12}$$

Furthermore, all second order partial derivatives of $\ell(\theta; x, y)$ with respect to θ_i, $i = 1, \dots, 6$ contain partial derivatives of the form

$$\begin{aligned} \frac{\partial}{\partial \theta_i}\Big(\frac{R_1(D_\theta)}{D_\theta}\Big) &= \frac{\partial}{\partial x}\left(\frac{R_1(x)}{x}\right)_{x = D_\theta} \cdot \Big(\frac{\partial D_\theta}{\partial \theta_i}\Big) \\ &= \frac{1}{D_\theta^2}\Big[R_2(D_\theta) - R_1^2(D_\theta)\Big]\left(A_\theta(x)\frac{\partial A_\theta(x)}{\partial \theta_i} + B_\theta(y)\frac{\partial B_\theta(y)}{\partial \theta_i}\right). \end{aligned} \tag{B.13}$$

In view of (B.9), $|R_2(D_\theta) - R_1^2(D_\theta)/D_\theta^2| \leq 1$ and $0 \leq R_1(D_\theta)/D_\theta \leq 1$ uniformly in $\theta \in K$. In addition, all moments of $X_1 - a$ and $Y_1 - b$ are bounded uniformly in $\theta \in K$, and

$$\sup_{\theta \in K} \mathbb{E}_\theta \left| A_\theta(X_1)\frac{\partial A_\theta(X_1)}{\partial \theta_i} + B_\theta(Y_1)\frac{\partial B_\theta(Y_1)}{\partial \theta_i} \right|^m < \infty, \quad \forall m > 1. \tag{B.14}$$

Combining (B.14), (B.13), (B.12) and (B.10) we obtain that

$$\sup_{\theta \in K} \mathbb{E}_\theta \left| \frac{\partial^2 \ell_1(\theta; X_1, Y_1)}{\partial \theta_i \theta_j} \right|^m < \infty, \quad \forall i, j = 1, \dots, 6,$$

i.e., condition (B.7) holds.

Verification of (B.8). It is sufficient to demonstrate that

$$\mathbb{E}_\theta \sup_{\theta \in K} \left| \frac{\partial^3 \ell_1(\theta; X_1, Y_1)}{\partial \theta_i \partial \theta_j \partial \theta_k} \right| < \infty, \quad \forall i, j, k = 1, \dots, 6. \tag{B.15}$$

First we note that

$$\frac{\mathrm{d}^2}{\mathrm{d}x^2}\Big(\frac{R_1(x)}{x}\Big) = \frac{\mathrm{d}}{\mathrm{d}x}\Big(\frac{R_2(x) - R_1^2(x)}{x}\Big) = \frac{1}{x^2}[R_3(x) - 3R_2(x)R_1(x) + 2R_1^3(x)].$$

Then it follows from (B.9) that $|\frac{\mathrm{d}^2}{\mathrm{d}x^2}[R_1(x)/x]| \leq 3$ for all $x \geq 0$. Differentiating (B.11), taking into account that

$$\sup_{\theta \in K} \mathbb{E}_\theta \left| \frac{\partial^2 u_i(\theta; X_1, Y_1)}{\partial \theta_j \partial \theta_k} \right|^m < \infty, \quad \sup_{\theta \in K} \mathbb{E}_\theta \left| \frac{\partial^2 v_i(\theta; X_1, Y_1)}{\partial \theta_j \partial \theta_k} \right|^m < \infty, \quad \forall i, j, k = 1, \dots, 6,$$

and applying the same reasoning as above we conclude that that (B.15) is fulfilled. ∎

B.3 Proof of Proposition 4.1

(a). Using representation (4.1), we have that

$$\mathrm{cov}_\theta(Z) = \rho^2 \mathrm{cov}_\theta(e_\varphi) + \mathrm{cov}_\theta(\varepsilon). \tag{B.16}$$

In addition, it follows from (A.6)-(A.7) that

$$\mathbb{E}_\theta(e_\varphi) = R_1(\varkappa) \begin{bmatrix} \cos\mu \\ \sin\mu \end{bmatrix} = R_1(\varkappa) e_\mu,$$

and from (A.8) - (A.9) that

$$\mathbb{E}_\theta(e_\varphi e_\varphi^T) = \begin{bmatrix} \mathbb{E}_\theta(\cos^2\varphi) & \mathbb{E}_\theta(\cos\varphi\sin\varphi) \\ \mathbb{E}_\theta(\cos\varphi\sin\varphi) & \mathbb{E}_\theta(\sin^2\varphi) \end{bmatrix} = \begin{bmatrix} \frac{1}{2} + \frac{1}{2}R_2(\varkappa)\cos(2\mu) & \frac{1}{2}R_2(\varkappa)\sin(2\mu) \\ \frac{1}{2}R_2(\varkappa)\sin(2\mu) & \frac{1}{2} - \frac{1}{2}R_2(\varkappa)\cos(2\mu) \end{bmatrix}$$

$$= \frac{1}{2}\begin{bmatrix} 1 + R_2(\varkappa)\cos(2\mu) & R_2(\varkappa)\sin(2\mu) \\ R_2(\varkappa)\sin(2\mu) & 1 - R_2(\varkappa)\cos(2\mu) \end{bmatrix}.$$

Then, after straightforward algebra,

$$\mathrm{cov}_\theta(e_\varphi) = \mathbb{E}_\theta(e_\varphi e_\varphi^T) - (\mathbb{E}_\theta e_\varphi)(\mathbb{E}_\theta e_\varphi)^T$$

$$= \frac{1}{2}\begin{bmatrix} 1 + R_2(\varkappa)\cos 2\mu & R_2(\varkappa)\sin 2\mu \\ R_2(\varkappa)\sin 2\mu & 1 - R_2(\varkappa)\cos 2\mu \end{bmatrix} - R_1^2(\varkappa)\begin{bmatrix} \cos^2\mu & \cos\mu\sin\mu \\ \cos\mu\sin\mu & \sin^2\mu \end{bmatrix}$$

$$= \frac{1}{2}\begin{bmatrix} 1 - R_1^2(\varkappa) + (R_2(\varkappa) - R_1^2(\varkappa))\cos 2\mu & (R_2(\varkappa) - R_1^2(\varkappa))\sin 2\mu \\ (R_2(\varkappa) - R_1^2(\varkappa))\sin 2\mu & 1 - R_1^2(\varkappa) - (R_2(\varkappa) - R_1^2(\varkappa))\cos 2\mu \end{bmatrix}.$$

Recalling that $\mathrm{cov}(\varepsilon) = \sigma^2 I$ and combining this with (B.16) we complete the proof of part (a). The proof of part (b) is immediate from (4.2).

(c). Let $\zeta \in [0, 2\pi)$ be a fixed number, and consider random variable $e_\zeta^T Z$. The variance of $e_\zeta^T Z$ is

$$\mathrm{var}_\theta(e_\zeta^T Z) = \rho^2 \mathrm{var}_\theta(e_\zeta^T e_\varphi) + \mathrm{var}_\theta(e_\zeta^T \varepsilon) = \rho^2 \mathrm{var}_\theta(e_\zeta^T e_\varphi) + \sigma^2.$$

Because

$$\mathbb{E}_\theta\left(e_\varphi^T e_\zeta\right) = \mathbb{E}_\theta\left(\cos(\varphi - \zeta)\right) = R_1(\varkappa)\cos(\mu - \zeta),$$
$$\mathbb{E}_\theta\left((e_\varphi^T e_\zeta)^2\right) = \mathbb{E}_\theta\left(\cos^2(\varphi - \zeta)\right) = \tfrac{1}{2} + \tfrac{1}{2}\mathbb{E}_\theta\left(\cos(2(\varphi - \zeta))\right) = \tfrac{1}{2} + \tfrac{1}{2}R_2(\varkappa)\cos(2(\mu - \zeta)).$$

we obtain that

$$\begin{aligned} \mathrm{var}_\theta(e_\zeta^T e_\varphi) &= \tfrac{1}{2} + \tfrac{1}{2}R_2(\varkappa)\cos(2(\mu - \zeta)) - R_1^2(\varkappa)\cos^2(\mu - \zeta) \\ &= \tfrac{1}{2}\big(1 - R_1^2(\varkappa)\big) + \tfrac{1}{2}\big(R_2(\varkappa) - R_1^2(\varkappa)\big)\cos(2(\mu - \zeta)), \end{aligned}$$

and therefore

$$\mathrm{var}_\theta(e_\zeta^T Z) = e_\zeta^T \Sigma e_\zeta = \tfrac{1}{2}\rho^2\Big[1 - R_1^2(\varkappa) + \big(R_2(\varkappa) - R_1^2(\varkappa)\big)\cos(2(\mu - \zeta))\Big] + \sigma^2. \tag{B.17}$$

Because $R_2(x) - R_1^2(x) \le 0$ for all $x \ge 0$ by (A.5), the minimum of the right hand side in (B.17) over ζ is achieved at $\zeta = \mu$, i.e.

$$\min_{\zeta\in[0,2\pi)} \mathrm{var}_\theta(e_\zeta^T Z) = \min_{e_\zeta : \|e_\zeta\|=1} e_\zeta^T \Sigma e_\zeta = e_\mu^T \Sigma e_\mu = \tfrac{1}{2}\rho^2\big[1 - 2R_1^2(\varkappa) + R_2(\varkappa)\big] + \sigma^2,$$

Thus e_μ is the eigenvector of the covariance matrix Σ corresponding to the minimal eigenvalue $\lambda_{\min}(\Sigma)$. Similarly, the maximum of the right hand side in (B.17) is achieved at $\zeta = \mu - \pi/2$, so that $e_{\mu-\pi/2}$ is the eigenvector corresponding to the maximal eigenvalue $\lambda_{\max}(\Sigma)$. The proof is complete. ∎

B.4 Proof of Theorem 5.1

(a). The proof is divided in two parts. First, we observe that the value of $\widehat{T}_n$ depends on S_{xx}, S_{yy} and S_{xy}, which are location invariant. Hence we start with derivation of the asymptotic distribution of the random vector with components

$$\sum_{i=1}^{n}(X_i-a),\ \sum_{i=1}^{n}(Y_i-b),\ \sum_{i=1}^{n}(X_i-a)^2,\ \sum_{i=1}^{n}(Y_i-b)^2,\ \sum_{i=1}^{n}(X_i-a)(Y_i-b).$$

Then we use the delta–method for derivation of the asymptotic distribution of $\widehat{T}_n$.

Consider vector

$$W := \left(X-a, (X-a)^2, Y-b, (Y-b)^2, (X-a)(Y-b)\right),$$

and let W_i, $i=1,\dots,n$ be the independent copies of W. Using the central limit theorem we have

$$\sqrt{n}\left(\frac{1}{n}\sum_{i=1}^{n}W_i - \mathbb{E}_{\theta_0}(W)\right) = \sqrt{n}(\bar{W}-\mathbb{E}_{\theta_0}(W)) \xrightarrow{d} \mathcal{N}_5\left(0,\Sigma_W\right), \quad n\to\infty,$$

where $\mathbb{E}_{\theta_0}(W) = \left(0, \frac{1}{2}\rho^2+\sigma^2, 0, \frac{1}{2}\rho^2+\sigma^2, 0\right)$, and

$$\Sigma_W = \begin{bmatrix} \frac{1}{2}\rho^2+\sigma^2 & 0 & 0 & 0 & 0 \\ 0 & \frac{1}{8}\rho^4+2\sigma^2\rho^2+2\sigma^4 & 0 & -\frac{1}{8}\rho^4 & 0 \\ 0 & 0 & \frac{1}{2}\rho^2+\sigma^2 & 0 & 0 \\ 0 & -\frac{1}{8}\rho^4 & 0 & \frac{1}{8}\rho^4+2\sigma^2\rho^2+2\sigma^4 & 0 \\ 0 & 0 & 0 & 0 & \frac{1}{8}\rho^4+\sigma^2\rho^2+\sigma^4 \end{bmatrix}.$$

Computation of $\mathbb{E}_{\theta_0}(W)$ is evident, and the entries of Σ_W are computed as follows

$$\begin{aligned}
&[\Sigma_W]_{11} = \mathrm{var}_{\theta_0}(X-a) = \mathbb{E}_{\theta_0}((X-a)^2) = \tfrac{1}{2}\rho^2+\sigma^2,\\
&[\Sigma_W]_{22} = \mathrm{var}_{\theta_0}((X-a)^2) = \mathbb{E}_{\theta_0}((X-a)^4) - \left[\mathbb{E}_{\theta_0}((X-a)^2)\right]^2 = \tfrac{1}{8}\rho^4+2\sigma^2\rho^2+2\sigma^4,\\
&[\Sigma_W]_{33} = \mathrm{var}_{\theta_0}(Y-b) = \mathbb{E}_{\theta_0}((Y-b)^2) = \tfrac{1}{2}\rho^2+\sigma^2,\\
&[\Sigma_W]_{44} = \mathrm{var}_{\theta_0}((Y-b)^2) = \mathbb{E}_{\theta_0}((Y-b)^4) - \left[\mathbb{E}_{\theta_0}((Y-b)^2)\right]^2 = \tfrac{1}{8}\rho^4+2\sigma^2\rho^2+2\sigma^4,\\
&[\Sigma_W]_{55} = \mathbb{E}_{\theta_0}\left[(X-a)^2(Y-b)^2\right] = \tfrac{1}{8}\rho^4+\sigma^2\rho^2+\sigma^4,
\end{aligned}$$

and

$$\begin{aligned}
&[\Sigma_W]_{12} = \mathbb{E}_{\theta_0}(X-a)^3 - \mathbb{E}_{\theta_0}(X-a)\cdot\mathbb{E}_{\theta_0}(X-a)^2 = \mathbb{E}_{\theta_0}(X-a)^3 = \rho^3\mathbb{E}_{\theta_0}(\cos^3\varphi) = 0,\\
&[\Sigma_W]_{13} = \mathbb{E}_{\theta_0}[(X-a)(Y-b)] = \rho^2\mathbb{E}_{\theta_0}(\cos\varphi\sin\varphi) = 0,\\
&[\Sigma_W]_{14} = \mathbb{E}_{\theta_0}[(X-a)(Y-b)^2] - \mathbb{E}_{\theta_0}(X-a)\cdot\mathbb{E}_{\theta_0}(Y-b)^2 = \mathbb{E}_{\theta_0}[(X-a)(Y-b)^2]\\
&\qquad\qquad = \mathbb{E}_{\theta_0}\left[\rho\cos\varphi(\rho^2\cos^2\varphi+\eta^2)\right] = 0,\\
&[\Sigma_W]_{15} = \mathbb{E}_{\theta_0}[(X-a)^2(Y-b)] - \mathbb{E}_{\theta_0}(X-a)\cdot\mathbb{E}_{\theta_0}[(X-a)(Y-b)] = 0 \quad \text{[similarly to } [\Sigma_W]_{14}\text{]}\\
&[\Sigma_W]_{23} = \mathbb{E}_{\theta_0}[(X-a)^2(Y-b)] - \mathbb{E}_{\theta_0}(X-a)^2\cdot\mathbb{E}_{\theta_0}(Y-b) = 0,\\
&[\Sigma_W]_{24} = \mathbb{E}_{\theta_0}[(X-a)^2(Y-b)^2] - \mathbb{E}_{\theta_0}(X-a)^2\cdot\mathbb{E}_{\theta_0}(Y-b)^2\\
&\quad = \rho^4\mathbb{E}_{\theta_0}(\cos^2\varphi\sin^2\varphi) + \rho^2\sigma^2\mathbb{E}_{\theta_0}(\cos^2\varphi) + \rho^2\sigma^2\mathbb{E}_{\theta_0}(\sin^2\varphi) + \sigma^4 - \left(\tfrac{1}{2}\rho^2+\sigma^2\right)^2\\
&\quad = \tfrac{1}{4}\rho^4\mathbb{E}_{\theta_0}(\sin^2 2\varphi) + \rho^2\sigma^2 + \sigma^4 - \left(\tfrac{1}{2}\rho^2+\sigma^2\right)^2 = \tfrac{1}{8}\rho^4+\rho^2\sigma^2+\sigma^4-\tfrac{1}{4}\rho^4-\rho^2\sigma^2-\sigma^4 = -\tfrac{1}{8}\rho^4,\\
&[\Sigma_W]_{25} = \mathbb{E}_{\theta_0}[(X-a)^3(Y-b)] - \mathbb{E}_{\theta_0}(X-a)^2\cdot\mathbb{E}_{\theta_0}[(X-a)(Y-b)] = 0,\\
&[\Sigma_W]_{34} = \mathbb{E}_{\theta_0}(Y-b)^3 - \mathbb{E}_{\theta_0}(Y-b)^2\cdot\mathbb{E}_{\theta_0}(Y-b) = 0,\\
&[\Sigma_W]_{35} = \mathbb{E}_{\theta_0}[(Y-b)^2(X-a)] - \mathbb{E}_{\theta_0}(Y-b)\cdot\mathbb{E}_{\theta_0}[(Y-b)(X-a)] = 0,\\
&[\Sigma_W]_{45} = \mathbb{E}_{\theta_0}[(X-a)(Y-b)^3] - \mathbb{E}_{\theta_0}(Y-b)^3\cdot\mathbb{E}_{\theta_0}[(Y-b)(X-a)] = 0.
\end{aligned}$$

Now we apply the delta–method in order to derive the asymptotic distribution of $\widehat{T}_n$. Define the function $g : \mathbb{R}^5 \to \mathbb{R}^2$ by

$$g(x_1, x_2, x_3, x_4, x_5) = \begin{bmatrix} -x_1^2 + x_2 + x_3^2 - x_4 \\ 2x_5 - 2x_1 x_3 \end{bmatrix}.$$

With this notation

$$\begin{bmatrix} S_{xx} - S_{yy} \\ 2S_{xy} \end{bmatrix} = g\left(\bar{W}\right).$$

Under the null hypothesis $g\left(\mathbb{E}_{\theta_0}(W)\right) = (0, 0)$, and the matrix of partial derivatives of g is

$$D(x) := \begin{bmatrix} -2x_1 & 1 & 2x_3 & -1 & 0 \\ -2x_3 & 0 & -2x_1 & 0 & 2 \end{bmatrix} \;\Rightarrow\; D_0 := D\left(\mathbb{E}_{\theta_0}(W)\right) = \begin{bmatrix} 0 & 1 & 0 & -1 & 0 \\ 0 & 0 & 0 & 0 & 2 \end{bmatrix}.$$

Therefore by the delta–method

$$\sqrt{n}\begin{bmatrix} S_{xx} - S_{yy} \\ 2S_{xy} \end{bmatrix} \xrightarrow{d} \mathcal{N}_2(0, D_0 \Sigma_W D_0^T), \quad n \to \infty,$$

and

$$D_0 \Sigma_W D_0^T = \left(\tfrac{1}{2}\rho^4 + 4\sigma^2\rho^2 + 4\sigma^4\right) I = sI.$$

This completes the proof of (a).

(b). Under H_0 we have that $\mathbb{E}_{\theta_0}(X) = a$ and $\mathbb{E}_{\theta_0}(Y) = b$. In addition, observe that independently of the angle distribution the random variable $\sigma^{-2}[(X-a)^2 + (Y-b)^2]$ has non–central χ^2–distribution $\chi^2_2(\rho^2/\sigma^2)$ with two degrees of freedom and non–centrality ρ^2/σ^2. Thus,

$$\begin{aligned} \tfrac{1}{2}\mathbb{E}_{\theta_0}\left\{\left[\,(X-a)^2 + (Y-b)^2\,\right]^2\right\} &= \tfrac{1}{2}\sigma^4 \mathbb{E}_{\theta_0}\left\{\frac{1}{\sigma^2}\left[\,(X-a)^2 + (Y-b)^2\,\right]^2\right\} \\ &= \tfrac{1}{2}\rho^4 + 4\rho^2\sigma^2 + 4\sigma^4. \end{aligned}$$

This formula shows that $\widehat{M}_n$ is an unbiased and consistent estimator of the parameter s.

By the results of part (a) we have that

$$n\left((S_{xx} - S_{yy})^2 + 4S_{xy}^2\right) \xrightarrow{d} \left(\tfrac{1}{2}\rho^4 + 4\rho^2\sigma^2 + 4\sigma^4\right) \cdot \chi^2_2, \quad n \to \infty.$$

The law of large numbers implies that $\widehat{M}_n \xrightarrow{p} \frac{1}{2}\rho^4 + 4\rho^2\sigma^2 + 4\sigma^4$ as $n \to \infty$; then applying the Slutzky theorem we complete the proof. ∎

References

Al-Sharadqah, A. and Chernov, N, (2009). Error analysis for circle fitting algorithms. *Electron. J. Stat.* **3**, 886–911.

Amos, D. E. (1974). Computation of modified Bessel functions and their ratios. *Math. Comp.* **28**, 239–251.

Anderson, D. A. (1981). The circular structural model. *J. Roy. Statist. Soc. B* **43**, 131–141.

Anderson, T. W. (1976). Estimation of linear functional relationships: approximate distributions and connections with simultaneous equations in econometrics. *J. Roy. Statist. Soc. Ser. B* **38**, 1–36.

Beck, A. and Pan, D. (2012). On the Solution of the GPS Localization and Circle Fitting Problems. *SIAM J. Optimization* **22**, 108–134.

Berman, M. (1989). Large sample bias in least squares estimators of a circular arc center and its radius. *Comput. Vision Graphics Image Process.* **45**, 126–128.

Berman, M. and Culpin, D. (1986). The statistical behaviour of some least squares estimators of the center and radius of a circle. *J. Roy. Statist. Soc. B* **48**, 183–96.

Chan, N. N. (1965). On circular functional relationships. *J. Roy. Statist. Soc. B* **27**, 45–56

Chernov, N. (2010). *Circular and Linear Regression: Fitting Circles and Lines by Least Squares.* CRC Press, Boca Raton.

Chernov, N. (2011). Fitting circles to scattered data: parameter estimates have no moments. *Metrika* **73**, 373–384.

Chernov, N. and Ososkov G. (1984). Effective algorithms for circle fitting. *Comput. Phys. Commun.* **33**, 329–333.

Davies, R.B. (1977). Hypothesis testing when a nuisance parameter is present only under the alternative. *Biometrika* **64**, 247–254.

Delogne, P. (1972). Computer optimization of Deschamps' method and error cancellation in reflectometry. *Proc. IMEKO-Symp. Microwave Measurement*, 117–123.

Freeman, P. R. (1977). Thom's survey of the Avebury ring. *J. Hist. Astronom.* **8**, 134–136.

Ibragimov, I. and Hasminskii, R. 1981. *Statistical estimation. Asymptotic Theory.* Springer, New York.

Kanatani, K. and Rangarajan, P. (2011). Hyper least squares fitting of circles and ellipses. *Comput. Statist. Data Anal.* **55**, 2197–2208.

Kanatani, K., Sugaya, Y. and Kanazawa, Y. (2016). *Ellipse Fitting for Computer Vision. Implementation and Applications.* Synthesis Lectures on Computer Vision, 8. Morgan & Claypool Publishers, Williston, VT.

Kåsa, I. (1976). A circle fitting procedure and its error analysis. *IEEE Trans. Instr. Measurement* **1**, pp. 8–14.

Kiefer, J. and Wolfowitz, J. (1956). Consistency of the maximum likelihood estimator in the presence of infinitely many incidental parameters. *Ann. Math. Statist.* **27**, 887–906.

Landau M. (1987). Estimation of a circular arc center and its radius, *Comput. Vision Graphics Image Process.* **38**, 317–326.

Lindsay, B. (1980). Nuisance parameters, mixture models, and the efficiency of partial likelihood estimators. *Phil. Trans. Royal Soc. London. Series A, Math. Phys. Sci.* **296**, No. 1427, 639–662.

Mardia, K.V. and Jupp, P.E. (2000). *Directional Statistics.* John Wiley and Sons, Chichester.

Neyman, J. and Scott, E.L. (1948). Consistent estimates based on partially consistent observations. *Econometrica* **16**, 1–32.

Núñes, P., Vázquez-Martin, R., Bandera A., and Sandoval, F. (2008). An algorithm for fitting 2-D data on the circle: applications to mobile robotics. *IEEE Signal Process. Lett.* **15**, 127–130.

Pratt V. (1987). Direct least-squares fitting of algebraic surfaces. *Comput. Graphics* **21**, 145–152.

Segura, J. (2011). Bounds for ratios of modified Bessel functions and associated Turán-type inequalities. *J. Math. Anal. Applic.* **374**, 516-528.

Soni, R. P. (1965). On an inequality for modified Bessel hunctions. *J. Math. Phys.* **44**, 406-407.

Späth, H. (1996). Least-squares fitting by circles. *Computing* **57**, 179–185.

Taubin, G. (1991). Estimation of planar curves, surfaces, and nonplanar space curves defined by implicit equations with applications to edge and range image segmentation. *IEEE Trans. Pattern Anal. Mach. Intell.* **13**, 1115-1138.

Thom, A. (1955). A statistical examination of the megalithic sites in Britain. *J. Roy. Statist. Soc. A* **118**, 275-95

Watson G.N. (1944) *A Treatise on the Theory of Bessel Functions.* Second edition. Cambridge University Press.